MULTIWALL CARBON NANOTUBE (MWCNT) AS A SATURABLE ABSORBER FOR GENERATION OF HIGH Q-FACTOR IN ERBIUM DOPED FIBER LASER (EDFL)

SITI NADHIRAH BINTI MOHAMED HASSAN

INSTITUTE OF GRADUATE STUDIES
UNIVERSITY OF MALAYA
KUALA LUMPUR

2016

MULTIWALL CARBON NANOTUBE (MWCNT) AS A SATURABLE ABSORBER FOR GENERATION OF HIGH Q-FACTOR IN ERBIUM DOPED FIBER LASER (EDFL)

SITI NADHIRAH BINTI MOHAMED HASSAN

DESSERTATION SUBMITTED IN FULFILMENT OF THE REQUIREMENTS FOR THE DEGREE OF MASTER OF PHILOSOPHY

INSTITUTE OF GRADUATE STUDIES
UNIVERSITY OF MALAYA
KUALA LUMPUR

2016

UNIVERSITY OF MALAYA

ORIGINAL LITERARY WORK DECLARATION

Name of Candidate : Siti Nadhirah binti Mohamed Hassan

Registration/Matric No:HGG 130006

Name of Degree: Master of Philosophy

Title of Project Paper/Research Report/Dissert ation/Thesis ("this Work"): Multiwall Carbon Nanotube (MWCNT) As A Saturable Absorber For Generation Of High Q-Factor in Erbium Doped Fiber Laser (EDFL)

Field of Study: Photonic science

I do solemnly and sincerely declare that:

(1) I am the sole author/writer of this Work;
(2) This Work is original;
(3) Any use of any work in which copyright exists was done by way of fair dealing and for permitted purposes and any excerpt or extract from, or reference to or reproduction of any copyright work has been disclosed expressly and sufficiently and the title of the Work and its authorship have been acknowledged in this Work;
(4) I do not have any actual knowledge nor do I ought reasonably to know that the making of this work constitutes an infringement of any copyright work;
(5) I hereby assign all and every rights in the copyright to this Work to the University ofMalaya ("UM"), who henceforth shall be owner of the copyright in this Work and that any reproduction or use in any form or by any means whatsoever is prohibited without the written consent of UM having been first had and obtained;
(6) I am fully aware that if in the course of making this Work I have infringed any copyright whether intentionally or otherwise, I may be subject to legal action or any other action as may be determined by UM.

Candidate's Signature Date:

Subscribed and solemnly declared before,

Witness's Signature: Date:

Name:

Designation:

ABSTRACT

In this dissertation, we propose to fabricate a higher mechanical strength, polyvinyl alcohol (PVA), type of host material added to the multiwall carbon nanotubes (MWCNTs) powder to significantly increase the capability of Q-switched cavity to generate high energy pulses. MWCNTs-PVA polymer composites based thin film is sandwiched between two fiber ferrules as a saturable absorber. MWCNTs concentration of 1.25 wt.% in PVA shows a good consistency in generating pulsed laser in Q-switched regime with a maximum repetition rate of 34.3 kHz, shortest pulse width of 3.49 μs, maximum peak power of 11.69 mW and maximum pulse energy of 43.23 nJ, respectively. Then, 1.125 wt.% of MWCNT/PVA-based Q-switched erbium-doped fiber laser (EDFL) incorporating in laser cavity with a tunable bandpass filter (TBPF) as the wavelength mechanism to achieve a broadband tuning range is proposed and demonstrated. The tuning range of the generated Q-switched pulses covered a wide wavelength range of 50 nm, which spanned from 1519 nm to 1569 nm and corresponded to the S- and C-band regions. The highest pulse energy of 52.13 nJ was obtained at an output wavelength of 1569 nm, with a corresponding repetition rate of 26.53 kHz and pulse width of 6.10 μs, at the maximum power of 114.8 mW. The proposed system which integrates a MWCNTs-PVA based thin film as passive saturable absorber is economical, easy to fabricate and compatible for integration in laser cavity.

ABSTRAK

Dalam disertasi ini, kami mencadangkan dan menunjukkan kekuatan mekanikal yang lebih tinggi, polyvinyl alkohol (PVA) , sejenis hos bahan yang ditambah kepada serbuk berbagai lapis dinding tiub karbon nano (MWCNTs) untuk meningkatkan keupayaan kaviti dalam Q-suis untuk menjana tenaga denyutan yang tinggi. Komposi tpolimer MWCNTs/PVA berasaskan filem nipis yang diapit di antara dua gentian ferul sebagai penyerap tepu. Kepekatan MWCNTs sebanyak 1.25 wt. % di dalam PVA menunjukkan konsistensi yang baik dalam menjana denyutan laser dalam Q-suis rejim dengan masing-masing menunjukkan kadar pengulangan maksimum iaitu 34.3 kHz, lebar denyut terpendek 3.49 μs ,kuasa puncak maksimum 11.69 mW dan tenaga nadi maksimum 43.23 nJ. Selepas itu, 1.125 wt. % MWCNT / berasaskan PVA Q-switched serat erbium-didopkan laser (EDFL) yang penala jalur boleh laras (TBPF) sebagai pelarasan gelombang dan mekanisme penapisan untuk mencapai pelbagai penalaan jalur lebar adalah dicadangkan dan ditunjukkan. Pelbagai penalaan daripada denyutan dijana Q-suis meliputi julat panjang gelombang seluas 50 nm dari 1519 nm hingga 1569 nm dan meliputi kepada jalur kawasan S- dan C-. Tenaga nadi maksimum sebanyak 52.13 nJ telah diperolehi pada panjang gelombang keluaran 1569 nm, dengan kadar pengulangan yang maksimum 26.53 kHz dan lebar denyut 6.10 μs, pada kuasa maksimum 114.8 mW. Sistem yang dicadangkan ini yang mengintegrasikan filem nipis MWCNTs/PVA berasaskan penyerap tepu pasif adalah ekonomi, kemudahan fabrikasi filem nipis dan serasi untuk integrasi dalam laser kaviti.

ACKNOWLEDGEMENTS

Alhamdulillah, I had finished my research work within the dateline. First and foremost, I would like to give a token of appreciation to my supervisors, Profesor. Datuk Dr. Harith bin Ahmad and Dr. Mohd Zamani bin Zulkifli for their support, priceless guidance, ideas, criticisms, motivation, inspiration, and knowledge throughout my studies. Through this research, I have learnt to be more independent, not only to obtain good research but also can be applied in my daily life. I would like to convey my sincere thanks to all of my friends in Photonics Research Center for providing excellent discussion as well as giving helpful assistance throughout the progress of the research. Last but not least, I would like to express my great gratitude to my family, especially for my mom, Puan Kartini binti Ishak for her moral support ,encouragement and fully understanding, in order to make sure that I could finish this research till the end.

TABLE OF CONTENTS

LIST OF FIGURES

LIST OF TABLES

LIST OF SYMBOLS AND ABBREVIATIONS

ASE	:	Amplified Spontaneous Emission
CNT	:	Carbon Nanotube
CW	:	Continuous Wave
EDF	:	Erbium Doped Fiber
EDFL	:	Erbium Doped Fiber Laser
FBG	:	Fiber Brag Grating
LD	:	Laser Diode
MWCNT	:	Multiwall Carbon Nanotube
OC	:	Optical Coupler
OPM	:	Optical Power Meter
OSA	:	Optical Spectrum Analyzer
PC	:	Polarization Controller
PVA	:	Polyvinyl Alcohol
PEO	:	Polyethylene Oxide
SA	:	Saturable Absorber
SESAM	:	Semiconductor Saturable Absorber Mirror
SWCNT	:	Single Wall Carbon Nanotube
TBPF	:	Tunable Band Pass Filter
WDM	:	Wavelength Division Multiplexer

CHAPTER 1: INTRODUCTION

1.1 Background of Fiber Laser

In 1960, Theodore Maiman (Maiman, 1960) ascertained a remarkable discovery in the optical science, which was the first experimental demonstration of laser. Since then, this device has gained significant interest from many researchers. The first demonstration of a fiber laser was by Snitzer (1961). Many experimental works on fiber lasers have been reported by several researchers during the 1960s (Koester, 1964), 1970s, (Burrus, 1976) and early 1980s (Digonnet, Gaeta, & Shaw, 1986). Solid state lasers are optically pumped by flash lamps or arch lamps as these light pump sources are comparatively cheap and can provide very high powers. However, they lead to a fairly low power efficiency, moderate lifetime, and can supply only broad and incoherent light. Solid state lasers used crystals or glasses doped with rare earth or transition metal ions, or semiconductor lasers as the gain medium. Solid-state lasers have been dominating since a few decades in the generation of pulsed laser such as the CO2 laser, Ruby laser and He-Ne laser due to their reliability and long term stability. However, solid state lasers are difficult to operate and require higher cost of regular maintenance. The performance of solid state laser is limited by the thermal lensing and beam distortions due to heat accumulation in the gain medium.

As an alternative, fiber laser becomes a widespread where optical fiber is used as a waveguide of the laser output transmissions in order to obtain ultrafast fiber laser. Optical fiber consists of small core diameter approximately 8 μm with cladding to protect the inner core from any damages. The schematic diagram of optical fiber can be seen in Figure 1.1.

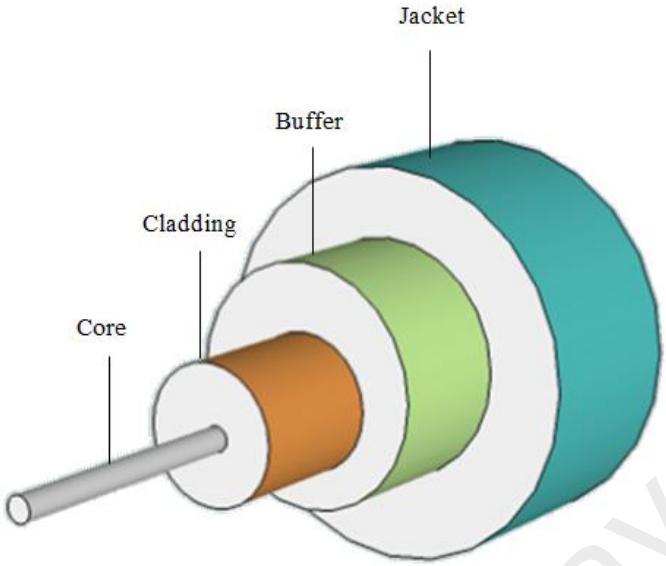

Figure 1.1: Schematic diagram of optical fiber

The optical fibers are more advantageous in terms of its capability to achieve higher optical efficiency and reliability rather than the solid state lasers while having more compact physical size. The size is crucial for applications such as materials processing, which might save the valuable factory floor space by reducing the amount of area that needs to be heated, cooled and rented. Furthermore, fiber laser lies in the flexible structure of the constituent optical fiber, which allows the pump signal to be coupled easily into the end of another fiber using connectors. Generally, fiber lasers are constructed with a gain medium of optical fiber doped with rare-earth elements such as ytterbium (1 micron region), erbium (1.5 micron region), and thulium (2 micron region).

1.2 Applications of Fiber Laser

Fiber lasers can be applied in wafer processing in the semiconductor industry. In the semiconductor processing industry, application of fiber laser is widespread, particularly for cutting and dicing silicon or other crystalline wafers on which integrated circuits have been fabricated. Cutting of silicon using a diamond saw has been common in the semiconductor industry. However, the diamond saw can cut only in straight lines and there can be problems with breakage while other methods tend to be slow or expensive. For 1.4 mm thick silicon, the cutting rate was measured at 0.7 m/minute. The cutting rate increases for thinner samples, reaching speeds greater than 6 m/minute for 0.5 mm thick samples. The cut edges were smooth with no cracking. Moreover, the fiber laser could cut in patterns other than straight lines. However, the laser cutting will cause thermal effects and eventually reduce the fracture strength. In conjunction with that matter, an investigation of the cutting of 50 micrometer thick silicon wafers by 700 femtosecond duration pulses of near infrared radiation from a fiber laser-amplifier combination was demonstrated and showed smooth walls with very little debris when the wafers were processed at a high scan speed and a high pulse repetition rate (500 kHz). Under the same processing conditions, the fracture strength of the cut wafers remained high. This was attributed to the very low heat effect that resulted from a femtosecond pulsed laser. These findings could lead to the use of fiber lasers for semiconductor processing in the future.

1.3 Research Objectives

Conventional laser pulse system has many shortcomings and limitations due to several barriers in term of complexity, size, and capability. Therefore, the objective of this work is to explore and investigate the capability and superiority of multiwall carbon nanotubes (MWCNTs) as a saturable absorber in upgrading the existing technology in realization of passive Q-switching operation. Multiwall carbon nanotubes (MWCNTs) have been a great candidate as a passive saturable absorber in Erbium-doped fiber laser (EDFL) system due to low cost and uncomplicated fabrication process. With the introduction of the MWCNTs polymer composite based passive saturable absorber, the search for polymer composite of the PVA as a host material will be investigated in this dissertation.

Therefore, the objectives are to:

1) characterize the optical properties of MWCNTs/PVA-based saturable absorber,
2) design an ultrafast EDFL which employs a MWCNTs/PVA-based saturable absorber to generate high energy pulses through Q-switching operation and,
3) design a tunable wavelength Q-Switched EDFL which employs MWCNTs/PVA-based saturable absorber.

CHAPTER 2: LITERATURE REVIEW

2.1 Introduction

This chapter begins with a brief overview of the theoretical background on erbium doped fiber (EDF) as the gain medium in the fiber laser. The theoretical part includes three-level energy diagram of erbium ions as an important aspect in optical amplification. This chapter also describes the photon generation by three common processes: absorption, spontaneous emission and stimulated emission. Then, this chapter also discusses the laser operation modes which can be categorized as continuous wave (laser) mode and pulse mode such as Q-switching and mode-locking. The focus is given to the Q-switching operation since the main objective is to obtain the high energy pulse in erbium doped fiber laser (EDFL).The Q-switching operation can be classified into active Q-switching, which uses external equipment in the cavity and passive Q-switching, which uses saturable absorber (SA). A brief description of the passive saturable absorber mechanism is presented in this chapter as it is more desirable than the active approach. This chapter will also cover the introduction of carbon nanotubes, which can be categorized to single wall carbon nanotubes (SWCNT) and multiwall carbon nanotubes (MWCNTs) as a saturable absorber and their useful optical properties in the EDFL.

2.2 Erbium doped fiber (EDF)

Erbium is one of the rare earth elements which have the appropriate energy levels in its atomic structure for light amplification at 1550 nm. The EDF has emerged as a strong candidate as the gain medium in the fiber laser, which provides desirable properties such as large gain bandwidth of typically tens of nanometers. Signal amplification in EDF is due to the excitation of the constituent erbium ions without introducing any effects of gain narrowing (Becker, Olsson, & Simpson, 1999; Mahad, Supa'at, &Sahmah, 2009), giving a significant interest for optical communication.

Besides EDF, there are many types of gain media such as semiconductor optical amplifier (SOA), Brillouin fiber amplifier (BFA) and Raman fiber amplifier (RFA). Though, the EDF is more preferable than these gain mediums for optical amplification in generating fiber laser.

A source of pump energy is provided by a diode laser and at three-level energy diagram for erbium ion (Er^{3+}) is shown in Figure 2.1. Optical amplification using EDFA occurs when the pump laser light from either a 980 nm or 1480 nm source laser excites the $Er^{3+}$from the ground state at level 1, denoted as ($^4I_{15/2}$).Then, the ions excite to an excited state at level 2 where the ions make a rapid, non- radiative decay to a long-life metastable state, denoted as $^4I_{13/2}$. The metastable state has a ~10^{-3}slifetime, which is a sufficient amount of time for optical amplification to occur. From there, the ions undergo spontaneous or stimulated emission to the lower-energy $^4I_{15/2}$ state. Finally, the optical output will be amplified by stimulated emission with wavelengths spanning from 1520 to 1560 nm. Hence, EDF is used due to the Erbium atoms having very suitable energy levels that absorb photons with a wavelength of 980 nm and decays to a metastable state equivalent to 1550 nm. This means that we can use any diode laser pump source at 980 nm and get a very high quality, and potentially very high power beam out at 1550 nm. Stimulated emission of radiation occurs when light in the 1550 nm travels through the erbium-doped fiber as shown in the next subsection.

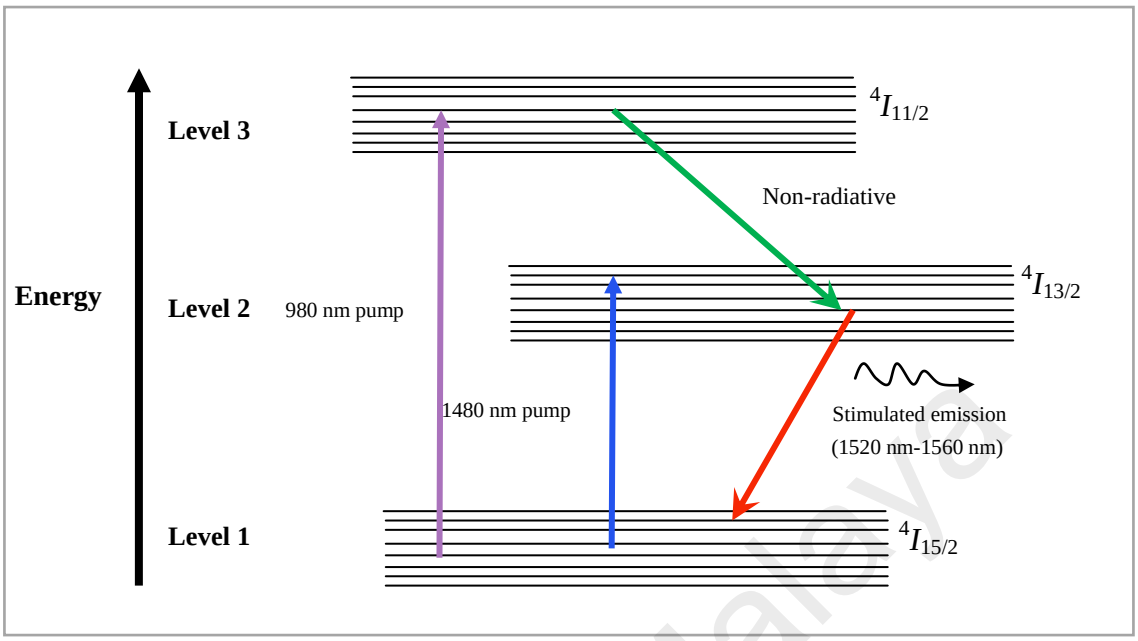

Figure 2.1: Three-level energy diagram for erbium ion (Er^{3+}) showing pump bands at 1480 nm and 980 nm.

2.3 Process of photon generation

Generation of photons in gain medium can be attained by getting through three processes which are absorption, spontaneous emission, and stimulated emission in order to get high intensity and in phase photons. Photons are excited and absorbed from the ground energy level (E_1) to a higher energy level (E_2) in the absorption process before experiencing spontaneous emission. Then, the photons are stimulated and emitted as an in phase and coherent photons in the gain medium as illustrated in Figure 2.2. Before stimulation emission happens, the photons go through relaxation time in the metastable state for ~10^{-3} s to build up population inversion as shown in Figure 2.3. After the population inversion in the gain medium is significantly build up, the photons will be stimulated as the laser output.

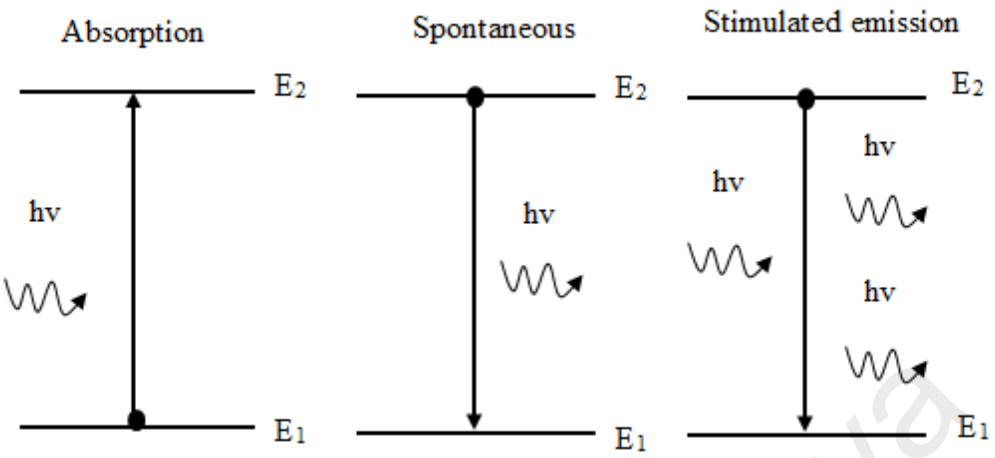

Figure 2.2: Process of photon generation

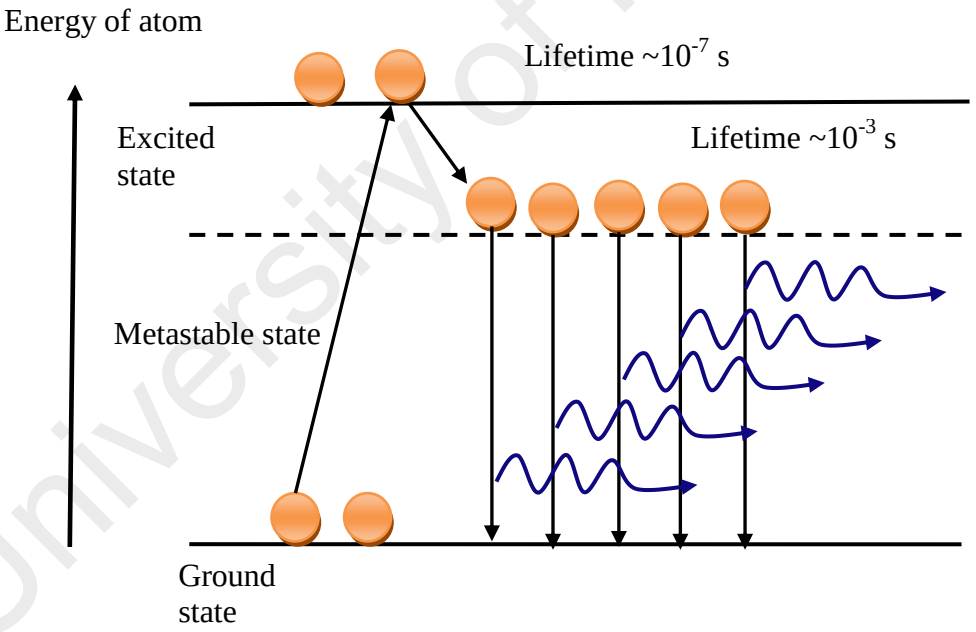

Figure 2.3: Population inversion process

2.4 Laser operation modes

In ultrafast fiber laser system, laser operations are divided into two modes which are continuous wave (CW) and pulse mode. CW laser is continuously pumped and emits light whereas pulse operation can be obtained by Q-switching and mode-locking techniques. Different types of energy source to pump (excite) the atoms from the gain medium which consequently emit dissimilar output laser. This pump can be electrical discharges, flash-lamps, arc-lamps, diodes and even light from another laser (optically pumped). In ultrafast fiber laser system, the lasing threshold starts in CW mode at a wavelength where the cavity gain to loss ratio is the highest as illustrated in Figure 2.4. Normally, the bandwidth of continuous wave at lasing threshold is only of a few nanometers of ~2 nm, whereas larger bandwidth can achieve approximately 20 nm when the cavity loss is switched to the high Q-factor and pulse will be formed.

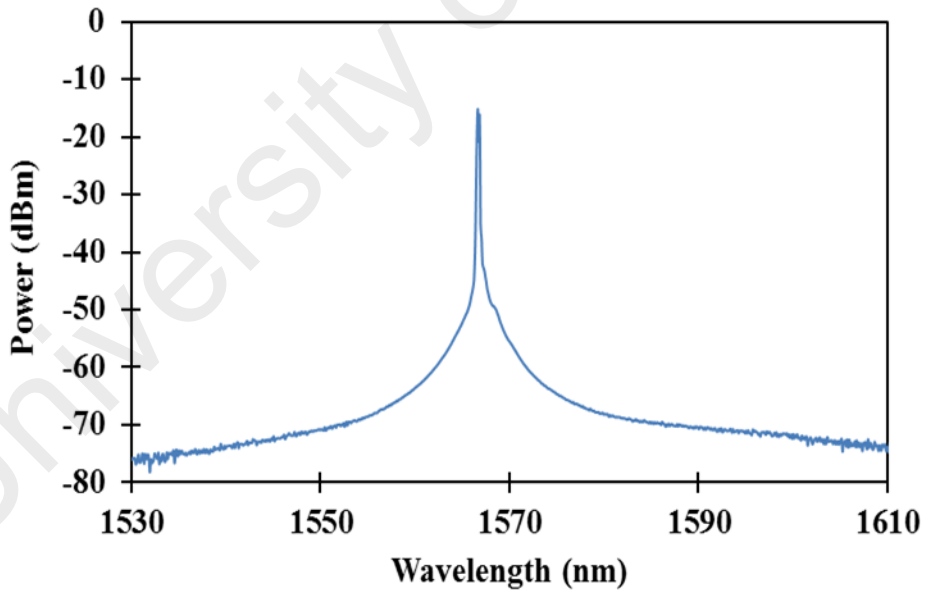

Figure 2.4: Spectrum of continuous wave (laser)

2.5 Q-switching operation

Q-switched pulsed operation can be defined as an enabling technique for pulsed laser operation which results from the large amount of energy stored in the gain medium released within a short time duration (Chen et al., 2014). The energy in the gain medium is largely built up by a pumping process and is initially prevented by a low Q factor due to the loss per oscillations which causes no feedback from the cavity. The higher Q factor will cause low loss in the oscillation round trip. This situation provides the buildup process of elevated population inversion and as laser operation can only occur by stimulated emission when the stored energy of the photons in the gain medium increases by the pumped energy. For continuous pumping, the gain medium should have a long upper-state lifetime to reach a high enough stored energy rather than losing the energy. In any case, the saturation energy should not be too low, because this could lead to excessive gain where the premature onset of lasing is more difficult to suppress. The loss from initial spontaneous emission or noise level in the laser cavity affects the stored energy in photons, and when it reaches the maximum level, this means the gain is getting saturated. At this point, the cavity loss is abruptly reduced or switched from high Q-factor to low Q-factor, consequently allowing the feedback in the cavity and the process of optical amplification by stimulated emission to begin. The intensity of the laser in the cavity is greatly increased and the rapid oscillation becomes sufficiently powerful that it begins to saturate or deplete within a very short time. The short pulse of laser light output from the laser is known as a 'giant' pulse. The peak power in the Q-switched giant pulse can be three or four orders of magnitude more intense than the continuous wave (CW) long pulse oscillation level created in the same laser using the same laser pumping rate (Mahad et al., 2009; Siegman, 1986).

The characteristics of Q-switched performances can be analyzed according to several parameters, such as the repetition rate, pulse width, pulse energy, and the average output

power. The measured Q-switched pulse repetition rate is usually as low as few kHz and pulse durations in the μs range. Compared to mode locked pulse operation, tendency of Q-switched operation to get pulse with higher energies can be observed and the pulse durations are also longer (Popa et al., 2011) as the time taken to replenish the extracted energy between two consecutive pulses depends on the lifetime of the absorbed photons in the gain medium which is typically in millisecond (ms) for erbium-doped fibers. In mode-locking approach, single pulse will be produced in a duration ranging from picoseconds to femtoseconds from fixing the random phase among the longitudinal modes of the laser cavity which is originating from the interference of cavity modes (Popa et al., 2011).

Q-switched pulse laser can be applied in applications that require pulses with long duration such as material processing, environmental sensing, range finding, medicine (Skorczakowski et al., 2010), and long-pulse nonlinear experiments (Laroche et al., 2002).Compared to mode locked pulse, Q-switched pulses exhibits more advantageous in terms of cost, efficient operation(a high output pulse energy to input power ratio), and easy integration into the laser cavity, whereas mode-locking concerns about the dispersion and nonlinearity parameters in the cavity in order to obtain stable operation.

2.5.1 Active Q-switched approach

In the case of active systems, the technique usually requires external equipment or external trigger such as the acousto-optic or electro-optic modulator (Kivisto et al., 2009; Williams, Jovanovic, Marshall, &Withford, 2010; Zhao et al., 2007) which can be rather complicated. The external equipment or trigger increases the complexity of the laser cavity due to the high insertion loss from the trigger. This drawback can be

mitigated by use of a passively Q-switched modulator, which is commonly referred to as a saturable absorber (SA).

2.5.2 Passive Q-switching

Passive Q switching is an alternative technique, where the active modulator is replaced by inserting the saturable absorber (SA) into the laser cavity and it does not require any additional equipment like active ones. An SA is an optical component with optical losses that diminish at high optical intensities and consequently allow the production of Q-switched pulses. Passive Q-switching approach is more desirable due to its advantages in terms of compactness, high reliability, low cost, and simple configuration. Hence, passive Q-switching has better features as it has more compact geometry and needs simpler setup configuration (Popa et al., 2011) in order to achieve stable pulse generation.

Earlier approach in the generation of Q-switched pulse utilizes semiconductor saturable absorber mirrors (SESAMs) incorporated into the fiber laser systems. Although this method works well in those systems, however, SESAMs have shortcomings in term of high fabrication cost, fragility, and a narrow tuning range, which is in the region of only a few tens of nanometers (Okhotnikov, Grudinin, &Pessa, 2004). SESAMs also require extra optical components such as lens and mirrors in the laser cavity in order to align the fiber output into the crystal and this introduce more complexity in the cavity design and a higher insertion loss (Huang et al., 2009). Furthermore, SESAMs have a lower optical damage threshold resulting to them of getting damage easily. Thus reduces their functional lifespan (Nelson, Jones, Tamura, Haus, &Ippen, 1997; S. A. Zhou, Ouzounov, & Wise, 2006).

2.6 Mechanism of Passive Saturable Absorber

Figure 2.5 shows the mechanism of passive saturable absorber in a laser cavity where the SA absorbs light in different degrees, depending on the optical intensity of the incident light. Incident light at low intensity is absorbed and excites carrier to the conduction band. When the incident light intensity increases, the conduction band becomes saturated due to occupy of electron in the conduction band, and no more states are available for carriers in the valence band to excite. By inserting the SA in the cavity, in each round trip, light will pass through the SA and it consists of low intensity with high loss and high intensity with low loss. This intensity contrast consequently causes the light starts to oscillate in pulse state.

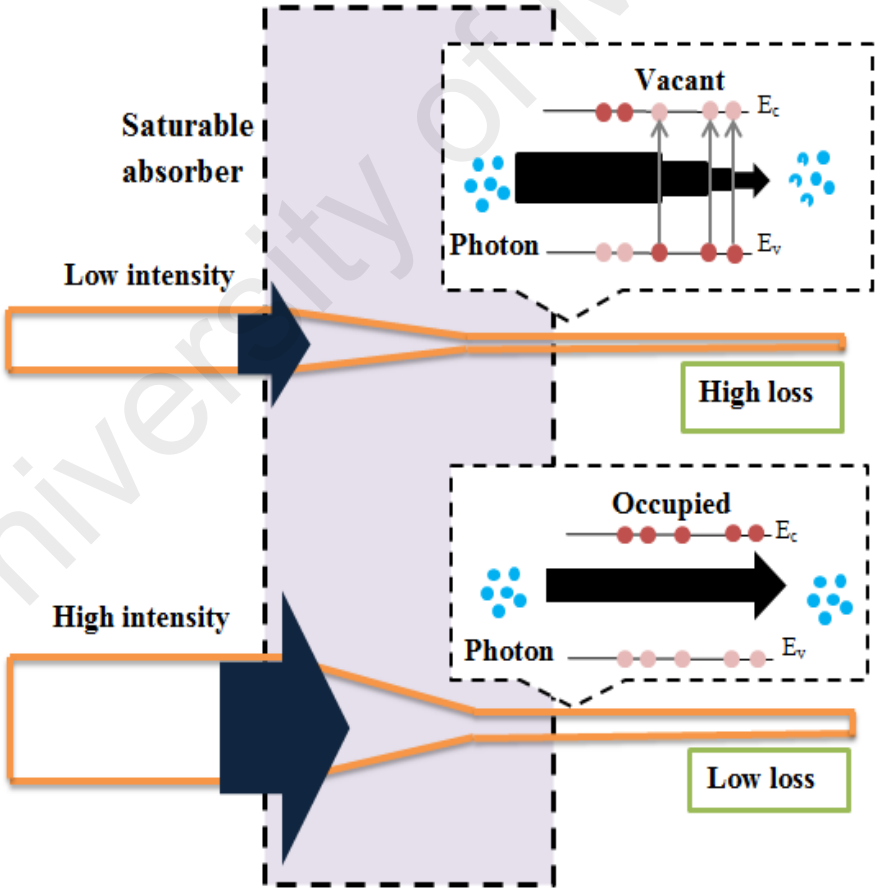

Figure 2.5: Mechanism of saturable absorber

2.7 Carbon Nanotubes based Saturable Absorber

Carbon nanotubes (CNTs) are long cylinders of covalently bonded carbon atoms. The carbon atoms are arranged in hexagonal network and each atom has three neighbors with which they form strong sp2 hybridized carbon-carbon atoms. CNTs are rolled-up carbon sheets that form seamless cylinders. Their electronic properties depend on their diameter and chirality, which is the twist angle along the tube axis. The density of states of single-walled CNTs is dominated by a series of characteristic van Hove singularities because of the one-dimensional nature of the electronic bands. Saturable absorption occurs when strong excitation depletes the electron population of the valence band and enhances the electron occupation of the conduction band. Semiconducting CNTs have a very fast recovery time, which is in a matter of picoseconds.CNT bundles exhibit faster dynamics (sub-picosecond) because of excited states relaxing through the metallic tubes. To a first-order approximation, the bandgap of CNTs, which is directly related to their optical absorption peak positions, varies inversely with their diameter. Thus, broadband operation is possible by using CNTs with a broad diameter distribution. Carbon nanotubes are linear structures that can reach microns of length with nano metric diameter. The CNTs can be divided into two types; the single wall (SWCNT) and the multi wall (MWCNT), which are presented in Figure 2.6. Single wall carbon nanotubes (SWCNTs) have numerous advantages such as ultrafast recovery time (Ismail, Ahmad, Harun, Arof, & Ahmad, 2013), low saturation intensity (Schibli et al., 2005), fast saturation absorption (Set, Yaguchi, Tanaka, & Jablonski, 2004a, 2004b) and ease of fabrication. SWCNTs work well at a particular wavelength, whereas operations in a wide-range of wavelengths require multiwall CNTs with different tube diameters (Popa et al., 2011). For instance, the diameter of SWCNT has to be 1-2 nm in the 1.5 μm operation regions (Ahmed et al., 2015). This factor places a limit on the usefulness of SWCNTs. For wideband operation, systems with an incorporated saturable absorber

having a gapless structure, such as graphene, have demonstrated in previous work (Zhang et al., 2010). Wideband graphene-based saturable absorber used in mode-locking (Sun et al., 2010) and Q-switching (Zhang, Zhuo, Wang, & Wang, 2012) are also demonstrated. Recent developments in CNTs, especially the fabrication of multiwall carbon nanotubes (MWCNTs), allow CNTs to perform similarly to graphene in a number of aspects, such as enabling a wide operating wavelength due to the multiple walls. The advantage of MWCNTs is larger saturation absorption than SWCNTs owing to the multiple walls of the MWCNTs. These multiple walls possesses higher molecular density weight per nanotubes and absorbs more light for each cavity round trip, consequently results in greater energy per pulse (Ahmed et al., 2015), representing a superior performance to that obtained using graphene (Ahmad, Muhammad, Zulkifli, & Harun, 2013).

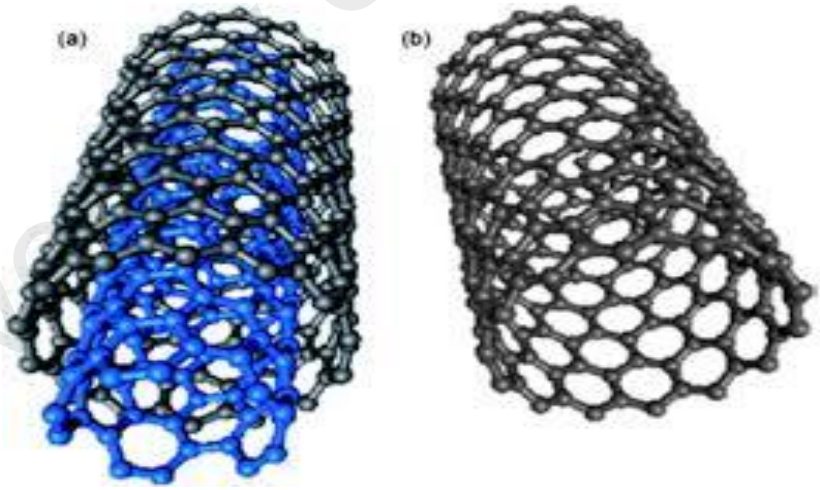

Figure 2.6: Structure of a) Multiwall carbon nanotubes (MWCNTs) and b) Single wall carbon nanotube (SWCNT) (Khin, Nair, Babu, Murugan, & Ramakrishna, 2012)

MWCNTs act as an SA in the laser cavity to modify the laser's continuous wave output into a train of short optical pulses. Ideally, the key requirements for such nonlinear optical materials are ultrafast recovery time, large nonlinearity, broad wavelength range, low optical loss, high power handling, cost-effective, and ease of integration into an optical system (Keller, 2003). These characteristics are attractive for future ultrafast photonic networks and can be used in ultrafast photonic devices, such as ultrafast all-optical switches and all-optical logic gates. Basically, CNTs shows great potential to perform as a good SA within the ultrafast fiber laser system. Table 2.1 shows the comparison of saturable absorber parameters between the single wall carbon nanotube (SWCNT) and multiwall carbon nanotube (MWCNT) and the results in reported works (Kamaraju et al., 2009; Lin, Yang, Liou, Yu, & Lin, 2013; Wang et al., 2008) and (Elim et al., 2004; Lim et al., 2006) have been summarized.

Table 2.1: Comparison of saturable absorber parameters of CNTs based saturable

Parameters	**SWCNT**	**MWCNT**
Modulation depth	~ 16 % (Wang et al., 2008)	~ 4.7% (Lin et al., 2013)
Saturation intensity, I_{sat}	~ 30 GW/cm^2(Kamaraju et al., 2009)	~ >100 GW/cm^2 (Elim et al., 2004; Lim et al., 2006)
Saturation fluence	~ 13.9 μJ/cm^2 (Wang et al., 2008)	~ 90 μJ/cm^2 (Lin et al., 2013)

From the table, it can be interpreted that SWCNT is a better saturable absorber compared to MWCNT in the aspect of higher modulation depth and low saturation intensity. The modulation depth of MWCNT is low due to the absorption changes between high and low intensity optical radiation (Yu, Grossiord, Koning, & Loos, 2007), and MWCNT possessed higher molecular density weight per nanotubes due to the multiple walls. Since the density of MWCNT is higher, it absorbs more light for each cavity round trip and consequently results in higher pulse energies. The value of saturation intensity for MWCNT in aqueous dispersion with ~ 40 nm outer diameters is higher than SWCNT, making the MWCNTs require higher irradiation intensity to reach absorption saturation (Elim et al., 2004; Lim et al., 2006). Therefore, MWCNTs have not been traditionally considered as SAs for passive mode locking (Hasan et al., 2014) while SWCNTs are more capable to achieve mode-locked operation. Nonetheless, SWCNTs still have shortcomings in terms of thermal characteristics and operating region.

2.8 Optical Properties of MWCNT

In ultrafast and compact fiber laser system, there are several optical properties that should be taken into account in order to produce high energy pulses especially in Q-switched operation. The MWCNTs based saturable absorber is capable to provide wideband operating region and higher saturation absorption. Furthermore, cost-efficiency is also vital in fabrication process so that a cheaper solution could be attained. This section discusses the optical properties of MWCNT that influence the performance of the cavity.

2.8.1 Wideband region

The operating wavelength ranges depend on the distribution of tube diameters of the CNT, which controls the bandgap (Zhang et al., 2011). MWCNT is structured by a multilayer of inner tube walls, which consists of sets of concentric cylindrical carbon sheet into the shape of a scroll. Figure 2.7 shows the typical diameter and inter wall distances of MWCNT is approximately 2 - 25 µm and 0.36 nm respectively, whereas the diameter of SWCNT is about 1-2 nm.

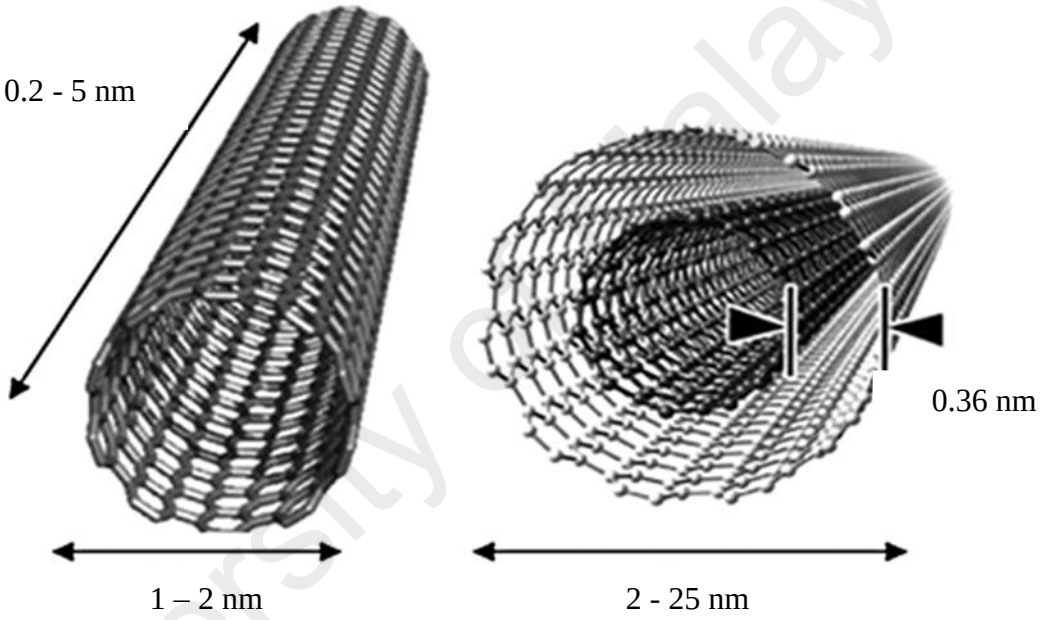

Figure 2.7: Diameter of carbon nanotubes a) SWCNT b) MWCNT (Reilly, 2007)

2.8.2 Polymer Composite as the Saturable Absorber Host Material

Polymer composite could assist the MWCNTs as a host material in the laser cavity. The selection of the polymer host material has an important impact on the system performance, and many possible host materials exist, such as polyethylene oxide (PEO) and polyvinyl alcohol (PVA).PVA was judged to offer the best solution due to its high solubility, high mechanical strength, better uniformity in thin film formation (Hassan & Peppas, 2000), and smoother surface compared to polyethylene oxide (PEO).

The PVA is a water-soluble synthetic polymer with monomer formula C_2H_4O, which has excellent film forming, emulsifying, and adhesive properties. It as well has high tensile strength, flexibility, high oxygen and aroma barrier, although these properties are dependent on humidity. The fabrication process and characterization of MWCNT/PVA saturable absorber was demonstrated in previous work (Ahmad et al., 2014). Table 2.2 summarized the results such as repetition rate, pulse width, average output power and pulse energy by using CNTs embedded with polymer composite as the host material. From the table, it can be seen that the PVA provides more mechanical strength and cooperates well with MWCNT in order to achieve better performance.

Table 2.2: Comparison of CNTs and polymer composite as a host material

Parameters of Q-switched	**SWCNT/PEO (Ahmed et al., 2015)]**	**MWCNT/PEO (Ahmad et al., 2014)**	**MWCNT/PVA (Ahmad et al., 2014)**
Pulse repetition rate (kHz)	16.6	22.2	29.9
Pulse width (μs)	8.00	8.80	3.49
Average output power (mW)	0.17	0.31	1.49
Pulse energy (nJ)	15.8	15.3	46.8

2.8.3 Higher saturation absorption

MWCNT exhibits a higher saturation absorption compared to the SWCNT due to its ability to absorb more photons per nanotubes based on the higher mass density of the multi-layer walls (Ahmad et al., 2014). Figure 2.8 demonstrates that the absorption band of CNTs is determined by the bandgap energies corresponding to the diameters of nanotubes and chirality (Sun, Hasan, & Ferrari, 2012), where the MWCNTs own larger absorption due to higher tube diameters. Theoretically, light is absorbed when the energy is suitable to that of the bandgap of an incident material, which means that a wide optical absorption is allowed if the bandgap energy distribution is also wide.

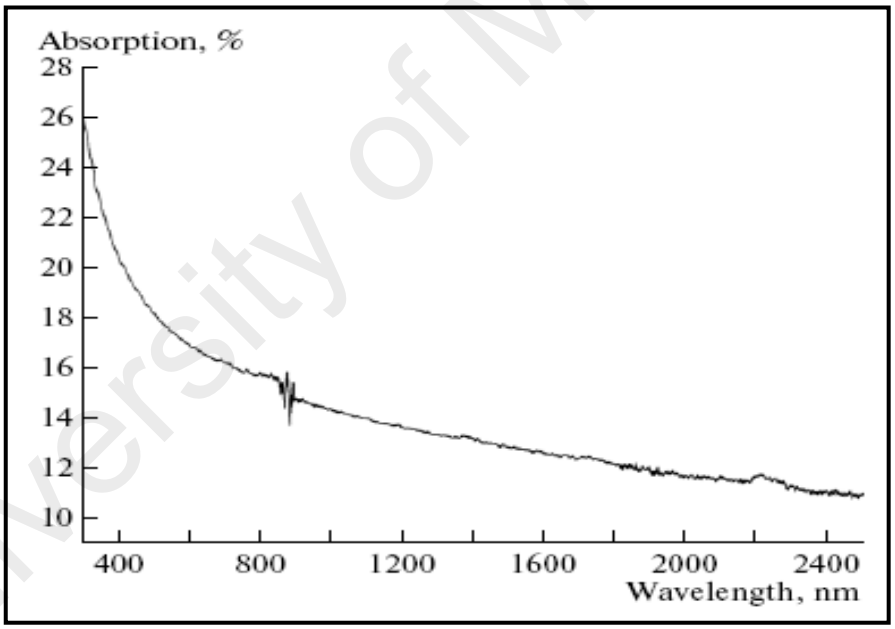

Figure 2.8: Linear absorption of MWCNTs based saturable absorber (Zhang et al., 2011)

2.9 Thermal Properties of MWCNT

High thermal damage threshold value, or in other words, capability to resist the saturable absorber from thermal damage is one of the concerns in compact ultrafast fiber laser system as it can subsequently improve the Q-switched laser performances. The thermal damage threshold of MWCNT is higher than that of the SWCNT (Ramadurai et al., 2008). Banhart (1999) reported that a damage threshold of 15.5 and 7.2 KW/cm^2 is achieved for MWCNTs and SWCNTs respectively. The multiple walls in MWCNT have advantage in protecting the inner walls from any thermal damage or oxidation process.

CHAPTER 3: MATERIALS AND METHODOLOGY

3.1 Introduction

This chapter describes the characterization of the multiwall carbon nanotubes (MWCNT) polymer based saturable absorber and the saturation absorption properties. The SA is characterized by using field emission scanning electron microscopy (FESEM) to observe the saturable absorber image and Raman spectroscopy to verify the SA characteristics. The saturable absorption properties are defined by nonlinear absorbance measurement, which is used to obtain the modulation depth of the SA, the saturation intensity and the non-saturable losses. This chapter also discusses the behavior of a fiber laser system with the employment of different coupling ratio. Furthermore, the effect of different pump power (by different laser diodes) on the laser threshold will be discussed. A description of experimental setups in various configurations will also be briefly covered in this chapter.

3.2 Characterization of Multiwall Carbon Nanotubes embedded in Polyvinyl (MWCNT/PVA)

The fabrication process of MWCNT embedded in polyvinyl alcohol (PVA) as the host material has been well demonstrated (Ahmad et al., 2014). In order to check the existence of the MWCNTs in the film, Field Emission Scanning Electron Microscopy (FESEM) and Raman spectroscopy (Ahmad et al., 2014) are used to observe its image and characteristics.

3.2.1 Field Emission Scanning Electron Microscopy (FESEM) Image

The dispersion state of MWCNTs in the PVA matrix is observed by using field emission scanning electron microscopy (FESEM). Figure 3.1 shows the FESEM image of the newly developed cross section of the MWCNT-PVA film. As observed, the MWCNTs are well-dispersed in the PVA matrix. In this work, the concentration of MWCNT used is 1.25 wt.%. The FESEM image does not reveal the structure of MWCNT distinctly due to the high concentration of PVA polymer. As can be seen from the figure, the circle-like structure is the round end nanotube observed in a cross-sectional view.

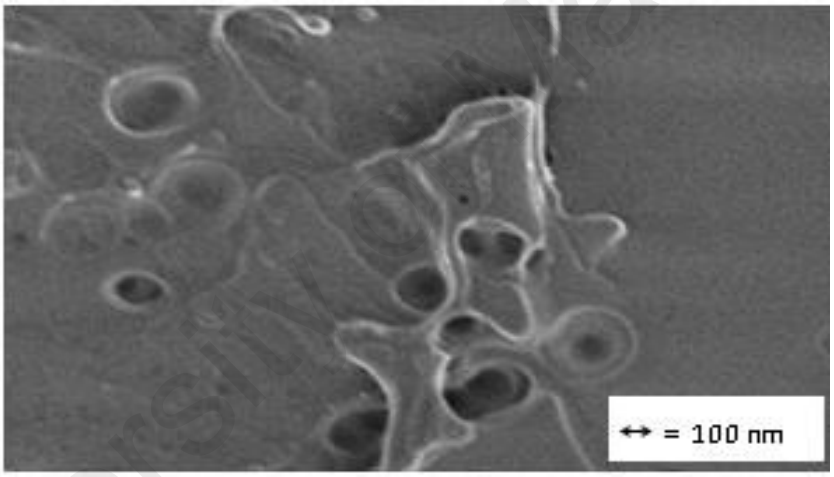

Figure 3.1: FESEM image of a MWCNTs/PVA film

3.2.2 Raman Spectroscopy

Figure 3.2 shows the Raman spectrum of a pure PVA film and MWCNTs-PVA based film. Raman spectrum of the pure PVA film is intense at 2915 cm^{-1}. As observed, the Raman spectrum of MWCNTs-PVA based film consists of various peaks at 1351 cm^{-1}, 1591 cm^{-1} and 2710 cm^{-1} which correspond to *D*, *G*, and *G'* bands. The Raman spectroscopy of the MWCNTs-PVA film is taken at 532 nm (2.33 eV) excitation in conjunction with 1800-lines/mm grating. The *D* band at 1351 cm^{-1} originates from a double resonance process and is attributed to the presence of amorphous disordered

carbon. The *G* band at 1591 cm^{-1} corresponds to tangential stretching C−C (carbon-carbon) vibrations on the nanotube wall plane (Kürti, Zólyomi, Grüneis, &Kuzmany, 2002; Saito et al., 2001). The *G'* peak at 2710 cm^{-1} originates from two-phonon scattering phenomena around the *K* point and around the *M* point in the Brillouin zone (Chakrapani et al., 2003). The intense peak at 2892 cm^{-1} is due to PVA host polymer. Apart from that, the radial breathing mode (RBM) which occurs at 100 to 500 cm^{-1} for SWCNTs is not observed due to restriction caused by the outer tubes of MWCNT.

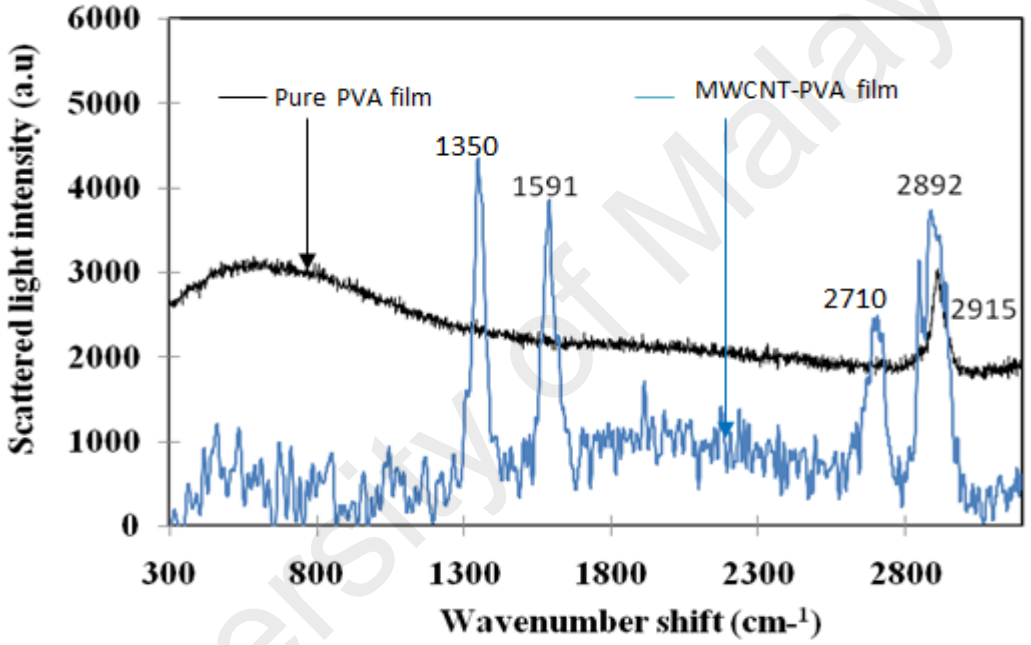

Figure 3.2: Unpolarized room temperature Raman scattering spectra of a pure PVA film (black curve)

3.2.3 Nonlinear saturable absorption

The nonlinear saturable absorption of a saturable absorber is commonly measured by using power-dependent absorption measurements where high intensity light 'bleaches' the material, and reduces the absorption, expressed as,

$$\propto \mathrm{I} = \frac{\propto_0}{\mathrm{I} + \mathrm{I}_{\mathrm{sat}}} + \propto_{\mathrm{ns}}$$

where $\propto$ (I), $\propto_0$, and $\propto_{\mathrm{ns}}$ are the intensity dependent absorption coefficient, the linear absorption coefficient, the non saturable absorption coefficient, respectively, whereas I and I_{sat} are the optical intensity and the saturation intensity, respectively. These measurements involve the optical source at certain wavelength is transmitted into the saturable absorber, and the changes in the induced optical loss is measured as a modulation depth. The modulation depth is thus the modulation amplitude in absorption or reflectivity which has a large influence in determining the performances of the saturable absorber. From the power-dependent absorption measurement, the saturation intensity and non-saturable losses can be verified. The saturation intensity is optical peak intensity that corresponds to a 50% reduction of the saturated part of its absorption (modulation depth), whereas the non-saturable losses can be defined as an undesirable portion of the loss, which is originates from defects in the saturable absorber. Figure 3.3 shows the nonlinear saturable absorption measurement that was carried out using a home-made femtosecond laser source (central wavelength: 1563.8 nm, repetition rate: 9.53 MHz, pulse duration: 610 fs). The result shows a modulation depth of ~6%, a saturation intensity of ~0.18 MW/cm^2 and non-saturable loss of 91%.

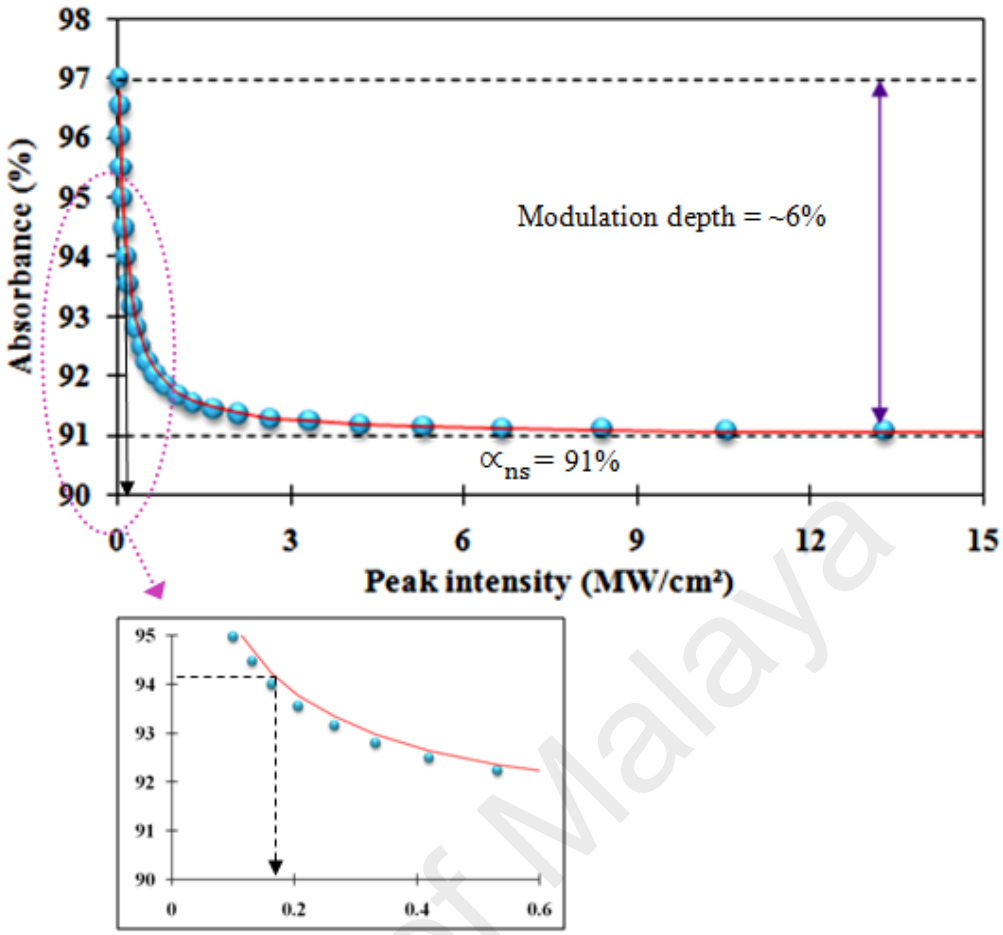

Figure 3.3: Nonlinear absorbance of MWCNT based PVA saturable absorber

3.3 Characterization of Erbium doped Fiber Laser (EDFL) System

The configurations in the erbium doped fiber laser system (EDFL) can be realized by employing commercial pump laser diode typically either a 1480 nm or 980 nm semiconductor laser diode as the pump, which is also known as a pump laser diode into the cavity in order to drive the power signal. Lasing pump power threshold is also different for each laser pump diode which correlates to the energy level of erbium ion, as discussed in Chapter 2. The output power is different depends on the required portion of the output, which is tapped out for analysis.

3.3.1 Laser threshold for different pump sources

In fiber laser, the pump sources that are commonly employed are laser diode at the wavelength of 1480 nm and 980 nm. Figure 3.4 shows the experimental setup for a laser design without the insertion of saturable absorber in the cavity. In this figure, 980 nm laser diode acts as the pump source where it pumps the light continuously. Then, it is connected to the wavelength division multiplexer (WDM) which couples the pump signals to the erbium doped fiber which is the gain medium. The optical signal will be amplified in the gain medium and passes through the isolator to ensure the unidirectional propagation of light. An optical coupler with the 90:10 ratio is used to extract 10% of the output to be analyzed while the other 90% stay in the cavity. Then the optical coupler is attached to the 1550 nm port of the WDM to close the circuit.

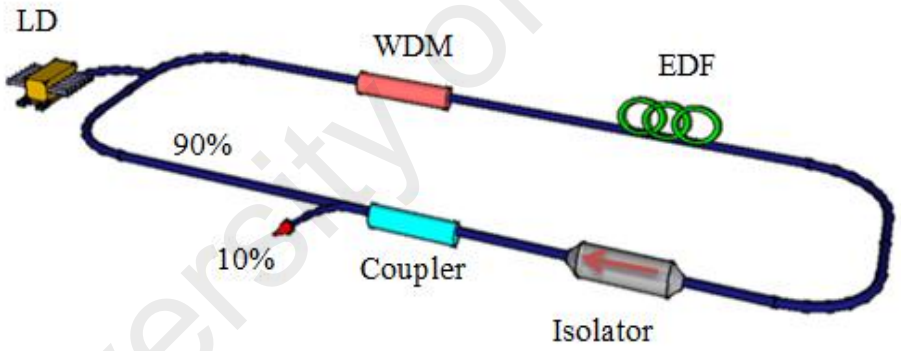

Figure 3.4: Experiment setup for laser output (without saturable absorber). Laser diode, LD, wavelength division multiplexer, WDM, erbium-doped fiber, EDF

Figure 3.5 shows the laser threshold before the insertion of saturable absorber in the cavity for different pump sources which are a) 1480 nm and b) 980 nm. Based on the Er^{3+} ion level energy diagram as discussed in Chapter 2, erbium ions from ground level 1($^4I_{15/2}$) absorb the energy and excited to upper level energy at level 2 ($^4I_{13/2}$)for pumping wavelength of 1480 nm and at level3 ($^4I_{11/2}$)for 980 nm. The erbium ions decay back to metastable state to build up the population inversion by non-radiative transition. Then, the ions will decay back to the 1.5 micron region and generate laser output.

The excited erbium ions at level 2 for pumping wavelength of 1480 nm will decay to the metastable state at level $^4I_{13/2}$,which is closely space to the wavelength of 1480 nm. This situation will result to a lower pump power laser threshold in continuous wave (laser) emission, giving a value of 9.45 mW, as illustrated in Figure 3.5 (a). The excited ions at level 3 for pumping wavelength of 980 nm are slightly far from the 1.5 micron region, giving higher threshold value of 15.5 mW to produce laser operation, as indicated in Figure 3.5 (b).The determination coefficient (R^2) value for the laser pump of 1480 nm is 0.9957 and 0.9994 for 980 nm as shown in Figure 3.5 (a) and (b), respectively. These values are close to one, indicating that the line is very linear where the laser cavity is in stable condition.

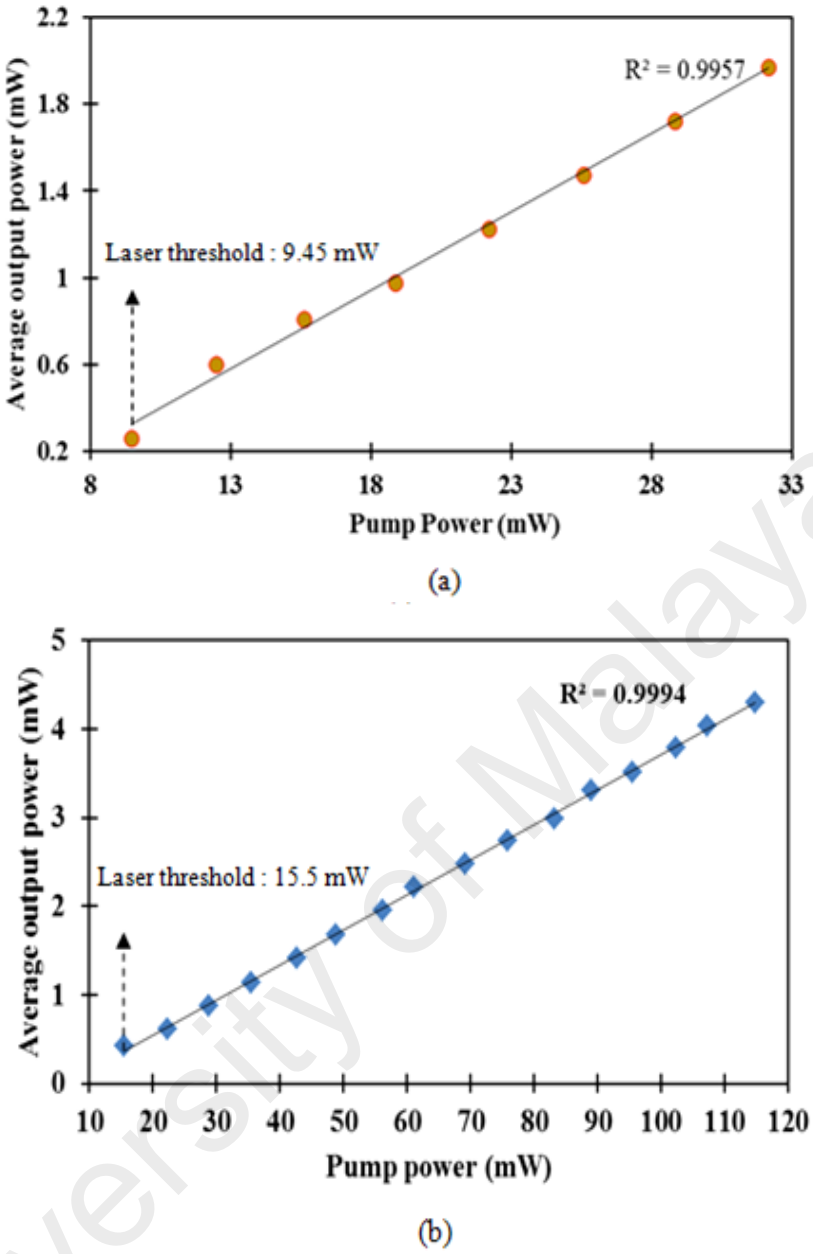

Figure 3.5: Laser threshold pump power without saturable absorber in the cavity for pump source a) 1480 nm and b) 980 nm

3.3.2 Different coupling ratio

Laser output can be determined by using a different coupling ratio such as 99:1, 95:5 and 90:10 where only 1%, 5% and 10% of the optical signal is tapped out for analysis, while another portion remains in the cavity. The laser output power for each coupler with a ratio of 99:1, 95:5 and 90:10 increases linearly when the pump power is raised. Figure 3.5 shows the linear graph of the different coupling ratio for different pump sources which are 1480 nm and 980 nm. In Figure 3.6 (a), a 1480 nm laser diode is used and the laser output efficiency (the pump power against the average output power) of each coupler is 1.47%, 5% and 8.68%, respectively. Figure 3.6 (b) shows the linear relationship between the pump power against the output power of the laser for each coupler ratio when a 980 nm laser diode is used as the pump source. The slope efficiency of the laser output with different optical couplers is 0.4%, 2.32% and 4.34% for the ratio of 99:1, 95:5 and 90:10 respectively. Based on both graphs, the average output power of the 1480 nm diode pumped laser is higher than 980 nm with the difference of approximately 0.9 mW for 1% output , 2.29 mW for 5% output and 3.76 mW for 10 % output, measured at the maximum pump power of 89.1 mW, as shown in Table 3.1

Table 3.1: Difference average output power between 1480 nm and 980 nm laser diode

Coupling ratio (%)	Difference of average output power (mW)
1%	0.9
5%	2.29
10%	3.76

Though 1480 nm pump source has higher optical power efficiency than 980 nm pump source, the latter is more desirable due to the 980 nm pump source has a narrower absorption spectrum, subsequently optimizing the laser cavity as it possesses less noise and low loss.

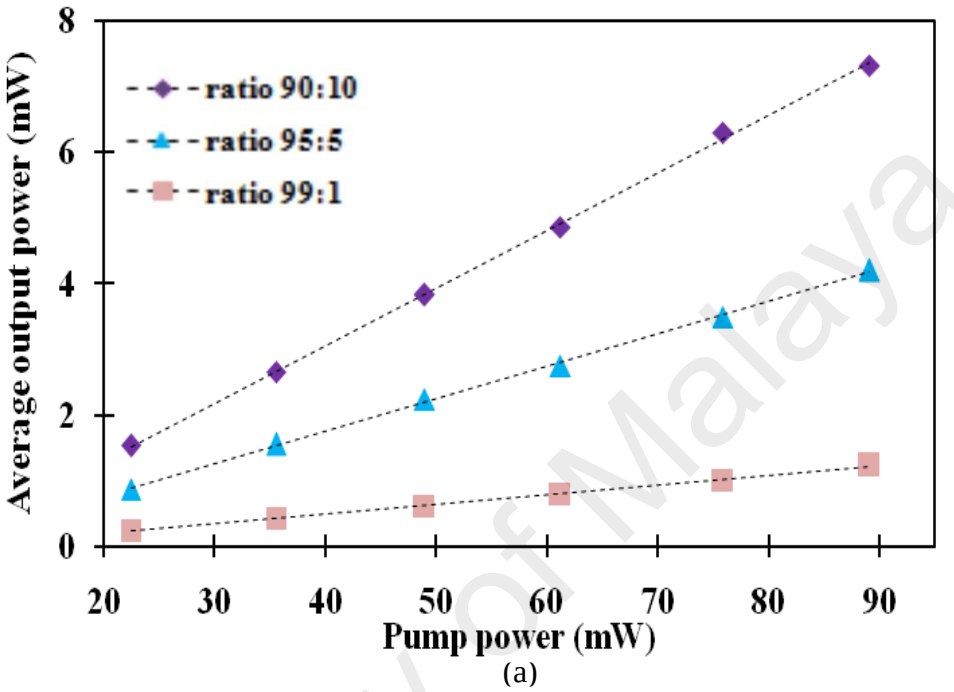

(a)

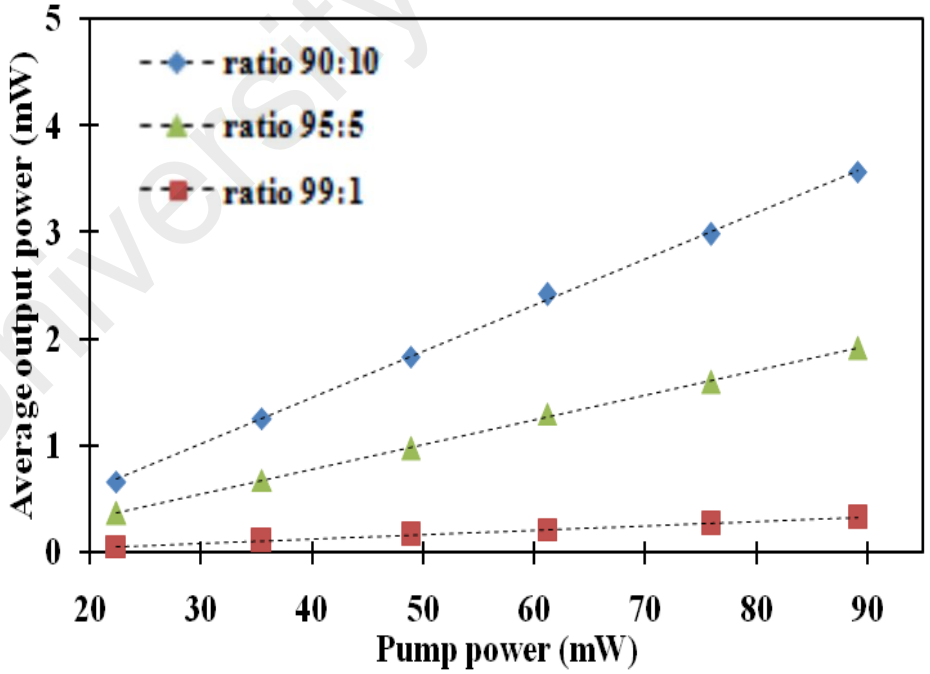

(b)

Figure 3.6: Pump power at different coupling ratio for pump source a) 1480 nm and b) 980 nm

3.4 Experimental Setup of Multiwall Carbon Nanotube (MWCNT)/ Polyvinyl Alcohol (PVA) as a Saturable Absorber in Passively Q-Switched Erbium doped Fiber Laser (EDFL)

Figure 3.7 shows the schematic of the experimental setup for the MWCNT-PVA based Q-switched erbium doped fiber laser (EDFL) in a ring configuration. It consists of a 4 m EDF (MetroGain-12) as the gain medium, which is pumped by a 1480 nm laser diode (LD) through a 1480 nm port of a fused 1480/1550 Wavelength Division multiplexer (WDM). Then, the EDF is connected to the input port of a polarization dependent isolator (PDI), which is an optical isolator to ensure the unidirectional oscillation within the cavity. A polarization controller (PC) is incorporated in the laser resonance cavity to optimize the Q-switching operation. The PC works as a retarder to maintain a given polarization state after each round trip. Next, the PC is connected to the saturable absorber, which is formed by sandwiching the 1.25 wt.% MWCNTA-PVA polymer composites in between two PC/FC connectors . The output of the MWCNTA-PVA based saturable absorber is then connected to the optical coupler with a ratio of 90:10 and to 10% portion of the signal in the cavity is tapped out for analysis. The other 90% of the signal remained in the cavity and is then channeled back to the 1550 nm port of the WDM and thereby completes the ring cavity. Spectral and temporal profiles of the output spectrum of the generated Q-switched pulses are measured by Yokogawa AQ6317 optical spectrum analyzer (OSA) with the resolution of 0.02 nm. A 500 GHz bandwidth Le Croy oscilloscope together with an Agilent 834440C Lightwave Detector is used to analyze the output pulse of the Q-switched pulses.

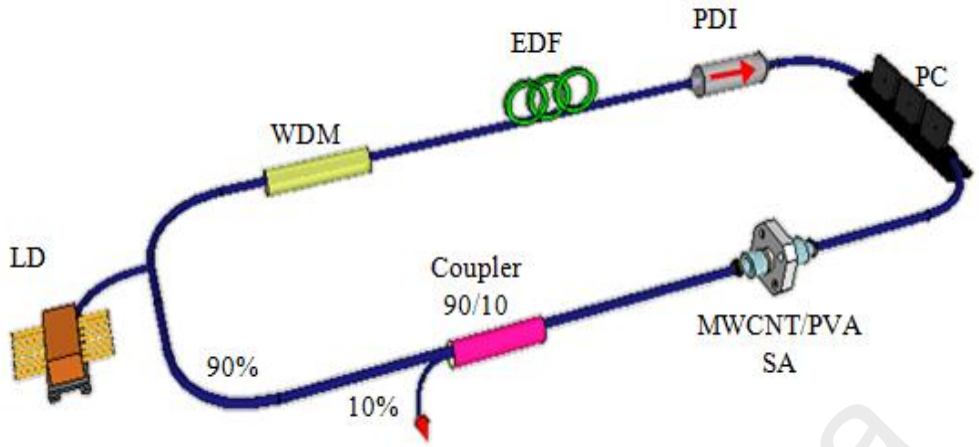

Figure 3.7: Schematic diagram for wavelength tuning in passively Q-switched fiber laser using an MWCNT/PVA SA. LD: laser diode, WDM: wavelength division multiplexer, EDF: erbium-doped fiber, PDI: Polarization dependent isolator, PC: polarization controller, MWCNT/PVA: Multiwall carbon nanotube/ polyvinyl alcohol

3.5 Experimental Setup of Tuning Range Characteristic of Q-Switched EDFL by a MWCNT/PVA based Saturable Absorber using TBPF as a Tuning Mechanism

The experimental setup of the wavelength tunable Q-switched fiber laser with MWCNT based SA is shown in Figure 3.8. The active medium was a 3 m long fiber that was highly doped with erbium and possessed absorption coefficients of 11dBm^{-1}at the wavelengths of 980 nm and 13dBm^{-1}at 1550 nm. A laser diode operating at 974 nm was used as the pump source, and was connected to the input port of a 980/1550 wavelength division multiplexer (WDM) that was then coupled to the erbium-doped fiber (EDF). The other end of the EDF was connected to an optical isolator at 1550 nm so as to ensure the optical signal traveled in the fiber acted as the host material. Then, the signal was channeled to the optical coupler (OC) with a ratio of 90:10.10% of the laser output was extracted for analysis using Yokogawa AQ6317 optical spectrum analyzer (OSA) with the resolution of 0.02 nm. A 500 GHz Le Croy oscilloscope together with a Thorlabs D400 FC InGaAs detector was used to analyze the pulse train of the Q-switched pulses. The other 90% of signal remained in the cavity and connected to the saturable absorber. In this experiment, the 1.125 wt.% MWCNT/PVA-based SA have a distributed diameter with the range of 10 to 20 μm, a length of 1 to 3 μm, and thickness of about 50 μm.The fabrication process was similar to the one reported in H. Ahmad et al.'s (2014). The other end of this SA was then connected to a Newport tunable bandpass filter (TBPF) to enable signal filtering, which performs as a wavelength selective device. The TBPF has a tuning range of 1519 nm to 1569 nm with a resolution of 0.05 nm, and this component was connected to the 1550 nm port of the WDM to close the loop.

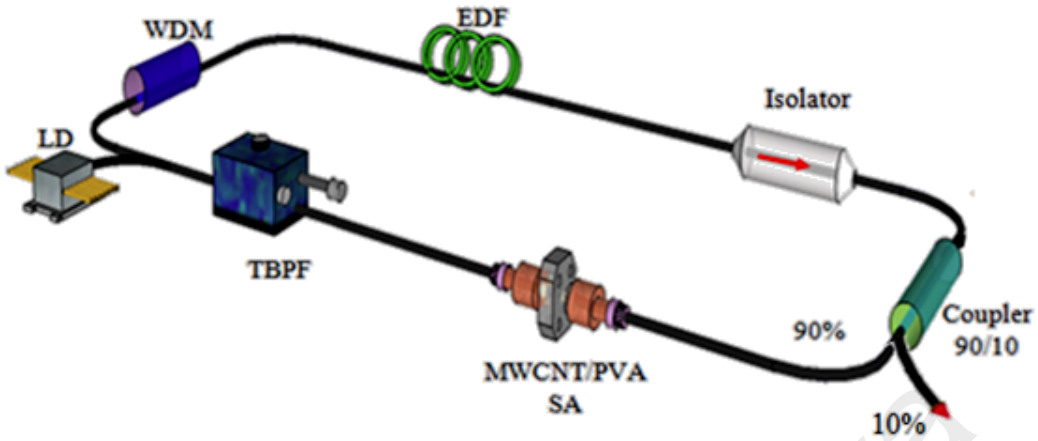

Figure 3.8: Schematic diagram for wavelength tuning in passively Q-switched fiber laser using an MWCNT/PVA SA. LD: laser diode, WDM: wavelength division multiplexer, EDF: erbium-doped fiber, MWCNT/PVA: Multiwall carbon nanotube/ polyvinyl alcohol, TBPF: tunable bandpass filter

CHAPTER 4: RESULTS AND DISCUSSION

4.1 Introduction

Recent developments in CNTs, especially the fabrication of multiwall carbon nanotubes (MWCNTs), allow CNTs to perform similarly to graphene as the saturable absorber in a number of aspects, such as enabling a wide operating wavelength due to the multiple walls. The advantage of MWCNTs is also a consequence of the large saturation absorption in comparison to SWCNTs, and provides for a higher pulse power as well as greater energy per pulse (Ahmed et al., 2015), which represents a superior performance to that obtained using graphene (Ahmad et al., 2013). This chapter discusses the outcomes of all experimental setup that are carried out to fulfill the objective of this research, which will also include all the explanation in detail. The performance of the developed Q-switched lasers will be described based on important parameters such as the pulse repetition rate, pulse width, average output power and energy pulses.

4.2 Multiwall Carbon Nanotube (MWCNT)/ Polyvinyl Alcohol (PVA) as a Saturable Absorber in Passively Q-Switched Erbium doped Fiber Laser (EDFL)

Figure 4.1 shows the comparison of the threshold of the laser without saturable absorber (continuous wave) and with saturable absorber (Q-switched operation) with respective values of 9.45 mW and 18.8 mW, with the corresponding slope efficiency of 7.5% and 5.6% respectively. The lower slope efficiency and the higher threshold for the laser system with saturable absorber are as expected due to absorption losses that occur when light travels into the saturable absorber with the loss percentage of approximately 1.9 %. A stable self-started Q-switched operation is achieved once the power reaches ~18.85 mW and is stabilizing at the maximum pump power of ~ 32.16 mW.

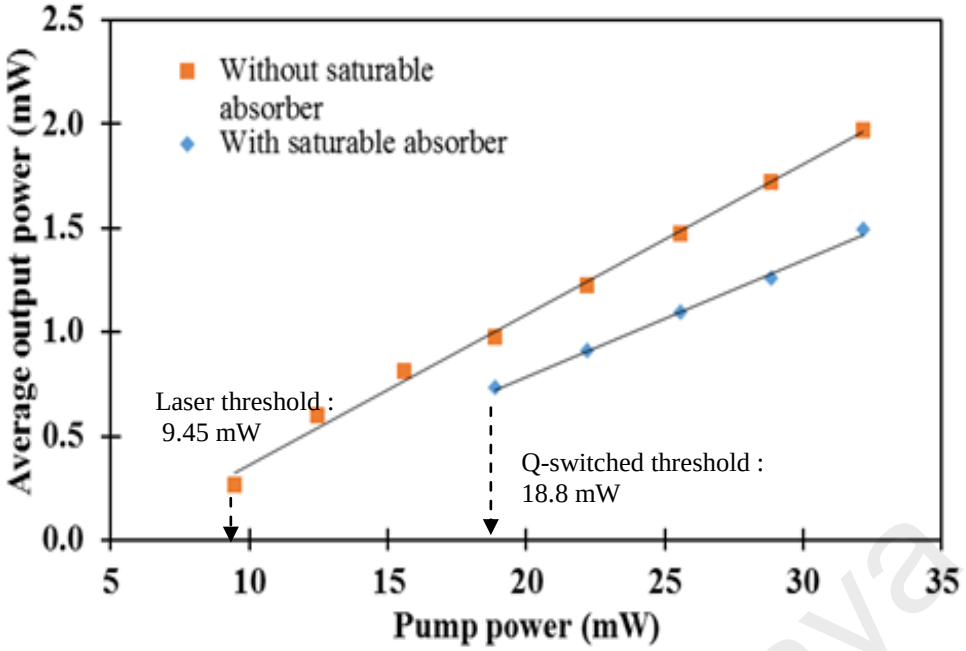

Figure 4.1: The lasing output power against the laser diode pump power at 1480 nm, giving a slope efficiency of 7.5% and 5.6 % for without (orange marker) and with (blue marker) saturable absorber within the laser cavity at different pump powers.

Figure 4.2 indicates the spectrum of Q-switched output pulse at various pump power starting from threshold lasing of 18.82 mW until the highest pump power of approximately 32.16 mW. During the Q-switched operation, raising the pump power will affect the stability of Q-switched pulse generation. This figure shows that the laser output exhibits spectral broadening with a central wavelength fixed at 1559.9 nm.

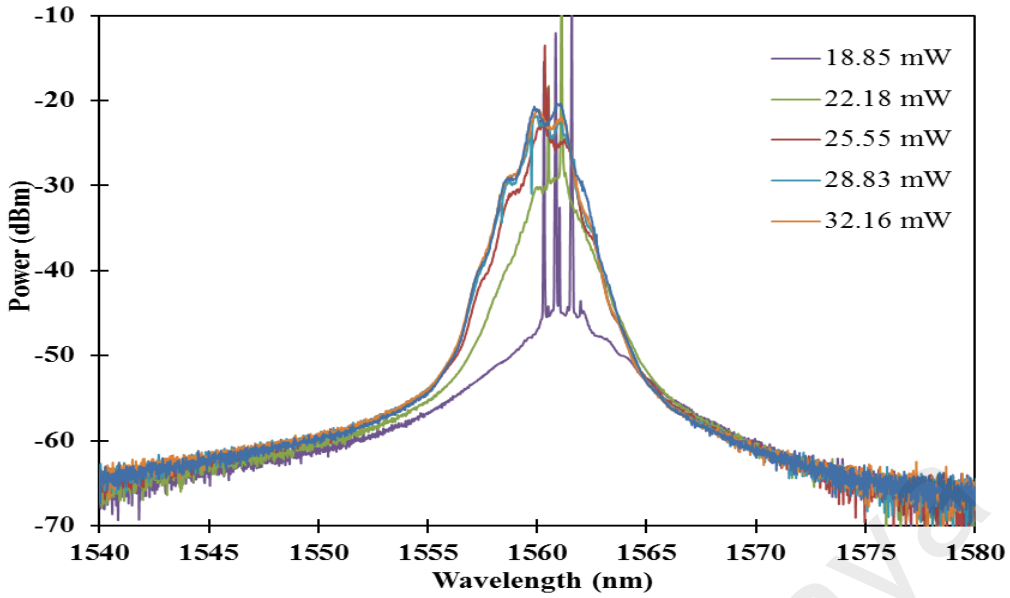

Figure 4.2: Spectrum of Q-switched output pulses for different pump powers.

The performance of CNT-based SA is not only dependent on its optical characteristics, but also on the design of the laser cavity. Although mode locking operation is capable to generate ultrashort pulses ranging from picosecond to femtosecond, their pulse energy is limited depends on the soliton theorem (Liu, Chow, Yamashita, & Set, 2013).The aim of this proposed work is to generate high pulse energies using these SA in EDFL system. The repetition rate of Q-switched fiber laser can be varied with reference to the lifetime of the gain medium as well as the pump power. Since different pump power induces different time required to replenish the extracted energy between two consecutive pulses, the detuning of repetition rate takes place (Yamashita et al., 2005), unlike with the passive mode locking regime where the repetition rate depends on the cavity length (Xinju, 2010). Figure 4.3 illustrates the pulse repetition rate and pulse width with respect to the pump power. The image shows that the repetition rate increases in a linear pattern against the pump power where it increases from 24.4 kHz at Q-switched threshold value of ~18.85 mW until a maximum value of 29.9 kHz at maximum Q-switched pump power of ~32.16 mW. In other hand, the pulse width behavior is in the opposite manner with repetition rate which falls as the pump power

increases. The pulse width of 7.06 µs decreases rapidly to 4.20 µs when the pump power of 18.85 mW increases to 22.18 mW. Then, the pulse width is eventually decreasing to the minimum value of 3.49 µs with the change of pump power from 22.18 mW to 32.16 mW. Once the pump power exceeds 32.16 mW, the pulse duration was kept at a constant value, probably because of the saturation of the upper energy level. Q-switching laser has a tunable repetition rate that is dependent on the cavity gain, loss and cavity birefringence. With the increase in the pump power, more electrons can be excited and accumulated in the upper energy level in the gain medium. The rise time and falling time of Q-switched pulse become simultaneously shorter, leading to the decrease of pulse width and the increase of repetition rate. Hasan et al. (2009) also reported that an effective way to obtain shorter pulse width is by using higher doped fiber and a shorter length of the laser cavity. Higher pump power induces shorter time to refill the extracted energy between the two successive pulses resulting in a higher repetition rate. However, in this experiment when the pump power is raised beyond 32.16 mW, the Q-switching pulsed starts to become unstable with noticeable amplitude variations and the output power starts to decrease.

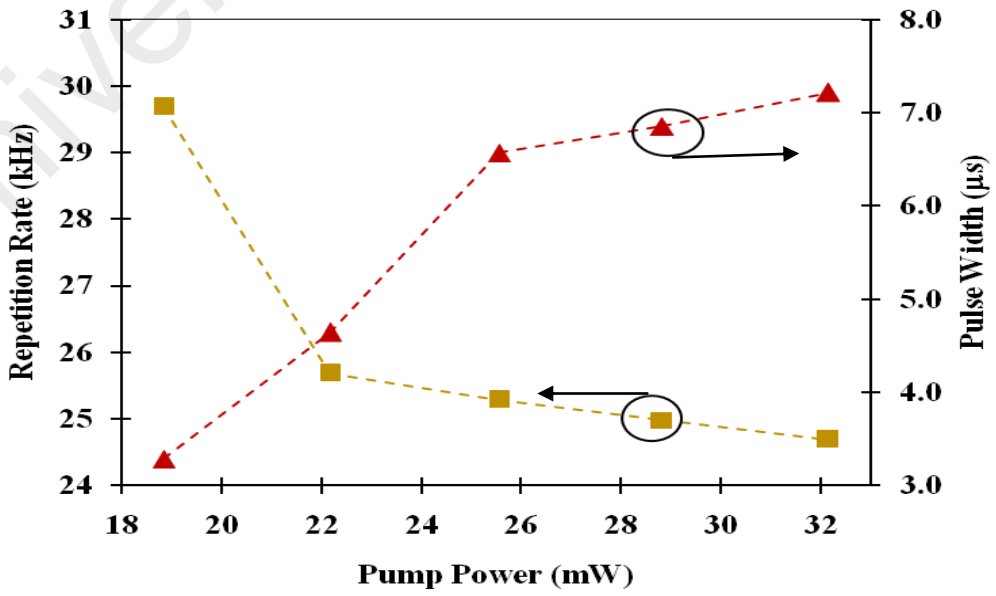

Figure 4.3: Pulse repetition rate and pulse width against pump power.

Figure 4.4 shows the change of average output power and pulse energy of Q-switched laser with respect to different pump power. One can clearly see that the average output power and pulse energy increase linearly against the pump power. At the pump power of 18.85 mW, the average output power and pulse energy are 0.73 mW and 29.9 nJ respectively. By continually increasing the pump power up to a maximum value of 32.16 mW, the average output power and pulse energy are 1.49 mW and 49.8 nJ, respectively.

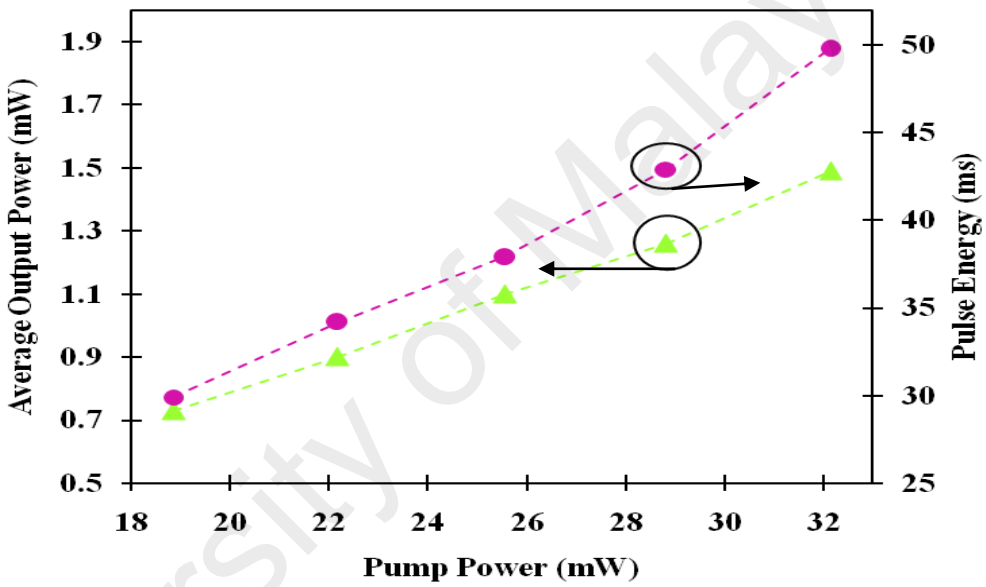

Figure 4.4: Pulse energy and average output power against pump power

In the stable operating regime, by continually increasing the pump power, the repetition rate gradually increases and the pulse train has a uniform intensity distribution with slightly fluctuation from peak to peak, as clearly depicted in Figure 4.5. In this figure, the full half-width maximum (FHWM) decreases as pump power increases from 18.85 mW to the maximum pump power of 32.16 mW. From the pulse train, it can be seen that there is no distinct amplitude modulation in each Q-switched envelop spectrum, which means that the self-mode locking effect is suppressed.

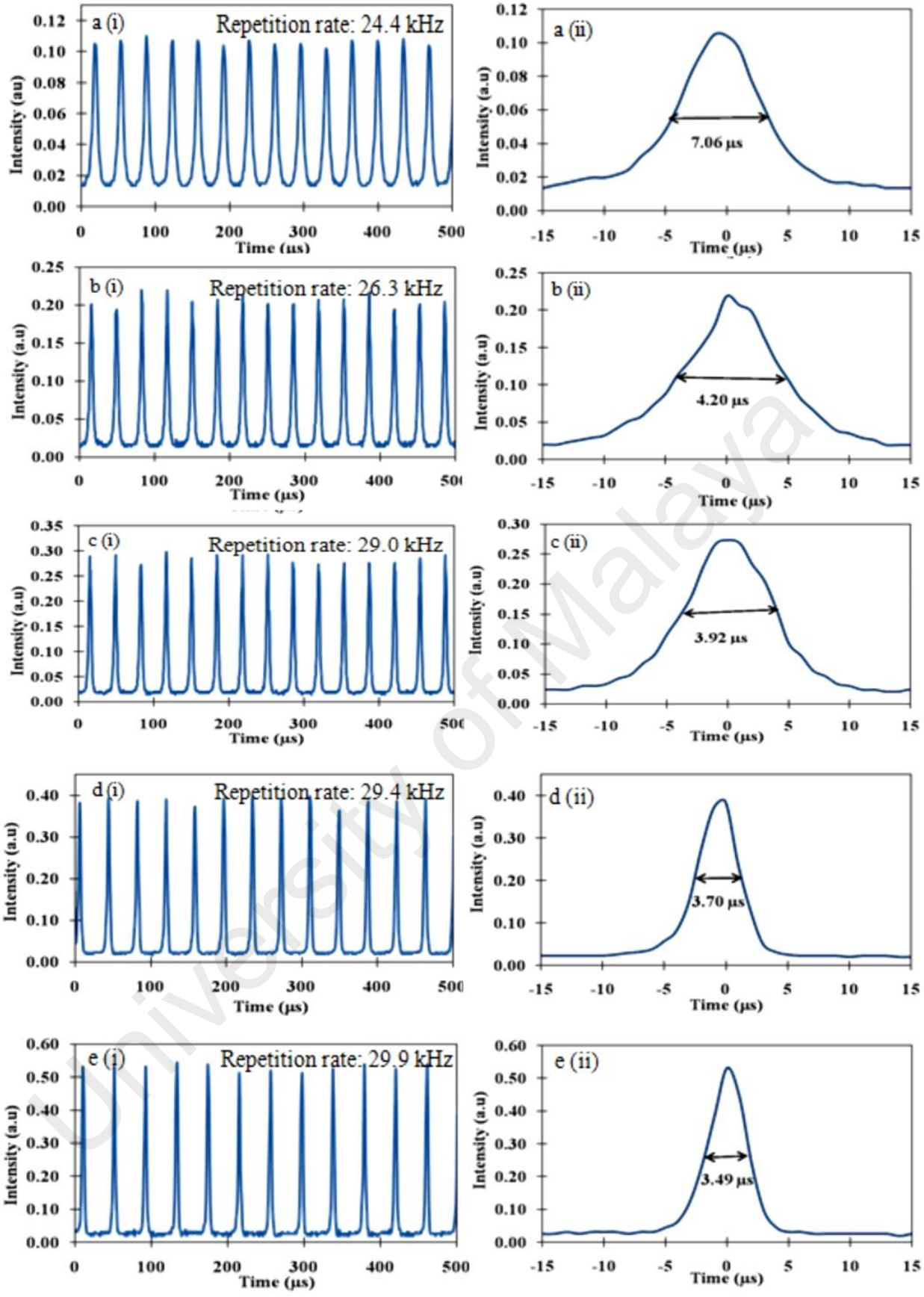

Figure 4.5: Pulse train (i) and envelop spectrum (ii) at different pump power a) 18.85 mW, b) 22.18 mW, c) 25.56 mW, d) 28.83 mW and e) 32.16 mW

4.3 Tuning Range Characteristic of Q-Switched EDFL by the MWCNTs/PVA-based Saturable Absorber using TBPF as a Filter Mechanism

Although Q-switched fiber lasers operating at a single wavelength have been used in many applications, considerable amount of interest exists the generation of tunable Q-switched fiber laser for areas such as spectroscopy (Chen et al., 2014), material processing, sensors, and communications (Han et al., 2014). Tunability has been demonstrated by using fiber Bragg gratings (FBGs) (Ahmad, Zulkifli, Muhammad, Zulkifli, & Harun, 2013; Dong, Liaw, Hao, & Hu, 2010; D. P. Zhou, Wei, Dong, & Liu, 2010),and also via an unbalanced Mach Zehnder interferometer with the assistance of a variable optical delay line (OVDL) in one arm (Han et al., 2014). For instance, tunable filter is an interesting wavelength selective mechanism for a relatively simple tunable Q-switched fiber laser as detailed in reference (Cao, Wang, Luo, Luo, & Xu, 2012). In those reports, the tuning range achieved is equal or less than 50 nm.

This experiment describes an easy technique for providing a passively Q-switched pulsed output with broadband wavelength tunability range using an erbium-doped fiber laser (EDFL) with an MWCNTs/polyvinyl alcohol (PVA)-based SA and tunable band pass filter (TBPF). The laser output carrying the Q-switched pulses covered a broadband tuning range of ~50 nm, which spanned from 1519 nm to 1569 nm. The highest pulse energy of 52.13 nJ was obtained at an output wavelength of 1569 nm with corresponding repetition rate of 26.53 kHz and pulse width of 6.10 μs at the maximum power of 114.8 mW. The laser and Q-switched thresholds were 15.5mW and 22.4 mW respectively.

So as to investigate the continuous wave operation of the laser, the system is tested without the insertion of saturable absorber to determine the minimum lasing threshold pump power, given a value of 15.5 mW. Then, the MWCNTs/PVA saturable absorber is

incorporated into the laser cavity, giving a lasing threshold of about 22.4 mW at the central wavelength of 1559 nm before the TBPF is incorporated in the system.

Figure 4.6 indicates the measured threshold pump power of the laser without and with saturable absorber which are 15.5 mW and 22.4 mW, respectively. The slope efficiency of the system without and with saturable absorber is 3.9% and 1.9%, respectively. The slope efficiency percentage with saturable absorber in laser cavity is lower, giving the power variation of about 2%, due to the insertion loss during the saturation absorption of the MWCNTs/PVA saturable absorber itself within the laser cavity.

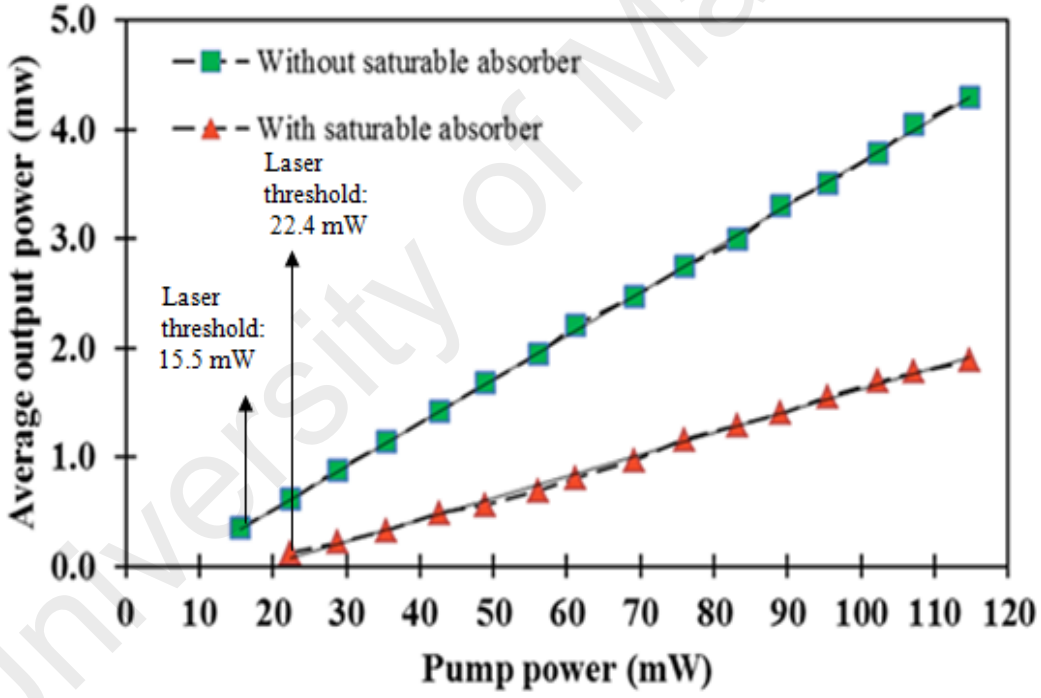

Figure 4.6: The lasing output power against the laser diode pump power at 980 nm, giving a slope efficiency of 3.9% for without (green marker) and 1.9% with (red marker) saturable absorber within the laser cavity at different pump powers

Figure 4.7 represents the output spectrum of the Q-switched pulses for different pump power before the insertion of TBPF into the cavity.The laser exhibits Q-switching at 1561.3 nm when the pump power increases from 22.4 mW and the laser central wavelength drifted to a shorter wavelength of 1559.84 nm as the pump power continuously increases to the maximum value of 114.8 mW. The measured line width at 3 dB was approximately 1.8 nm at a threshold pump power of 22.4 mW. An increase in pump power from 35.5 mW to 114.8 mW corresponded to the 3 dB line width increment from approximately 2 nm to 2.4 nm, as depicted in Figure 4.7.

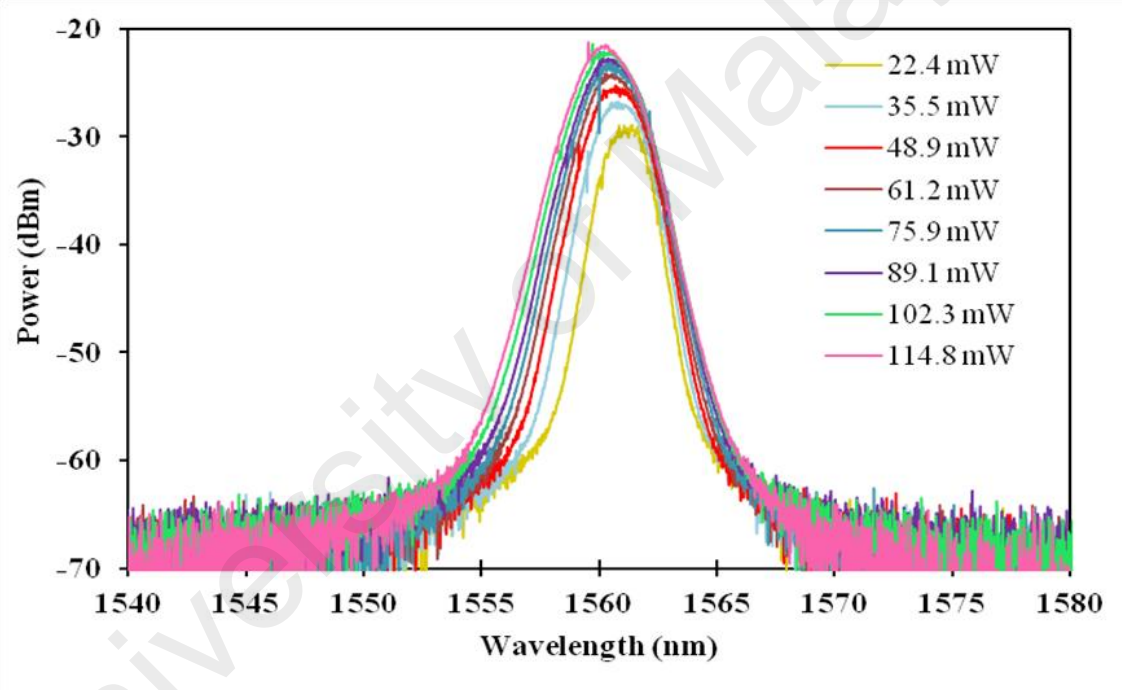

Figure 4.7: Output spectra of Q-switched operation for different pump powers before inserting TBF into the cavity

Figure 4.8 shows the variation of the peak wavelength against pump power. As can be observed, when pump power increases from 35.5 mW to 114.8 mW, the peak wavelength shifts linearly from 1561.3 nm to 1559.84 nm accordingly. The optical spectrum and peak wavelengths are shifted towards the shorter wavelength when the pump power is increased due to the rise in the erbium gain resulting to the shifting of the operating wavelength to a lower region (Rosdin, 2014).When the pump power is continuously increased beyond the maximum value, the pulse generation will eventually decrease at a certain level of gain. This is because the gain becomes smaller when the population inversion happens to all the erbium ions in the fiber, as explained by Rashid (2008).

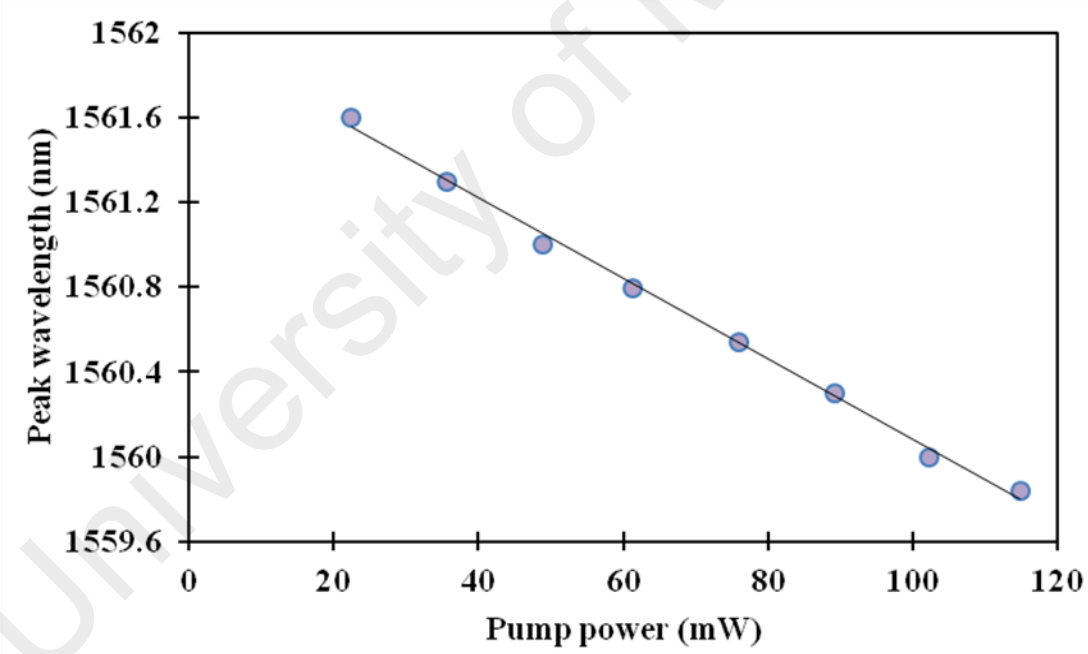

Figure 4.8: Variation of the peak wavelength of Q-switched output spectra against pump power

The various spectra of tuned output wavelengths when a TBPF was placed in the cavity are shown in Figure 4.9. Only six output wavelengths are shown in this figure to ensure clarity, although the entire set of measurements comprises of all wavelengths measured in increments of 0.05 nm (the smallest granularity permitted via the micrometer head of the TBPF) across the tuning range of about 50 nm from 1519 nm to 1569 nm. The measurements were taken at the maximum pump power of 114.8 mW. The range was limited by the TBPF tunability that spanned from 1520 nm to 1570 nm.A further limitation resulted from the amplified spontaneous emission (ASE) range of the utilized doped fiber, for which the ASE spectrum is represented by the dotted line in Figure 4.9. The variation of the output power was about 7 dBm, from an output power of -15 dBm (minimum) at 1519 nm to -8 dBm (maximum) at 1549 nm, when taking into account the peak results across the entire measured wavelength range.

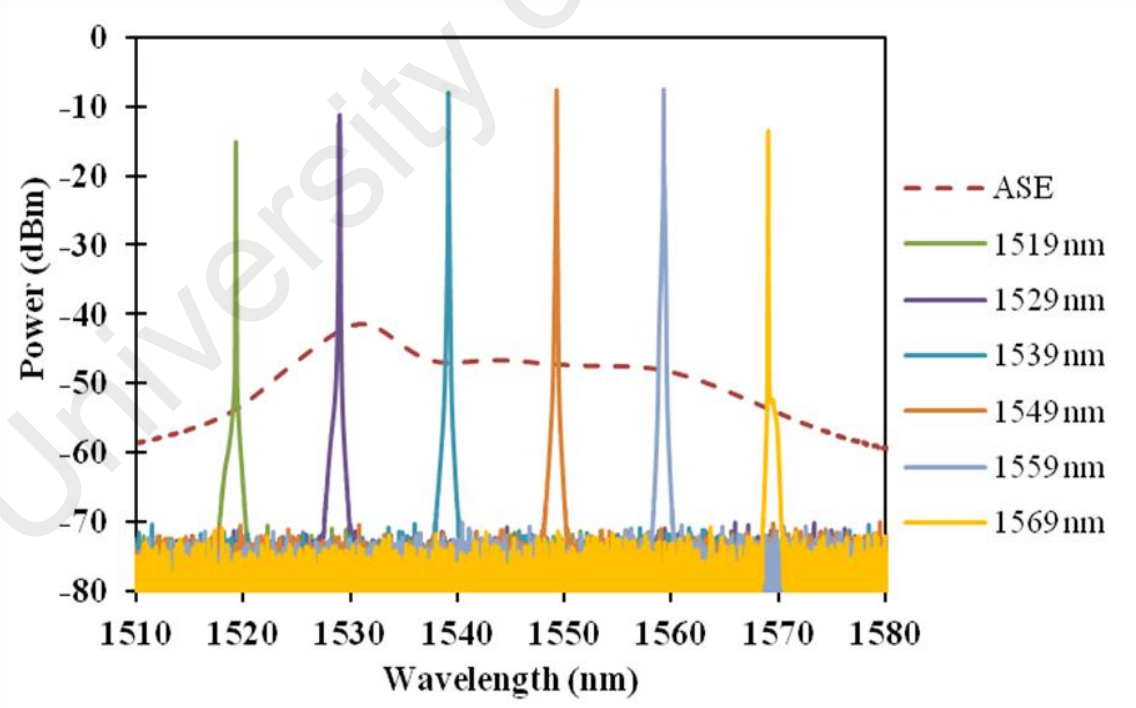

Figure 4.9: Output spectra of tunable Q-switched operation for six tuned wavelengths after inserting the TBPF

The measurements of pulse repetition rate, pulse width, average output power and pulse energy against pump power at different operating wavelength of 1529 nm, 1549 nm, and 1569 nm are indicated in Figure 4.10. Figure 4.10 (a) indicates the linear dependency between the pulse repetition rate and the pump power. The pulse repetition rate increases from 13.73 kHz to 47.68 kHz at 1529 nm, 5.70 kHz to 34.58 kHz at 1549 nm, and 5.02 kHz to 26.53 kHz at 1569 nm, in correspondence with the increase of pump power from 22.4 mW until 114.8 mW. There was an approximately 3-7 kHz increase in repetition rate for every increase of 10 mW in the pump power. In contrast to the pulse repetition rate having an approximately linear relationship with the pump power, the pulse width had a nonlinear decrease that can be noted in Figure 4.10 (b).The pulse width of this MWCNT/PVA-based tunable Q-switched EDFL decreased from a value 11.2 μs to 2.83 μs at output wavelength 1529 nm, 15.27 μs to 4.19 μs at 1549 nm, and 19.33 μs to 6.10 μs for 1569 nm, during an increase in pump power from 22.4 mW until 114.8 mW.

Figure 4.10 (c) and Figure 4.10 (d) indicate the average output power and pulse energy as a function of the pump power respectively, with measurements taken at different output wavelengths of 1529 nm, 1549 nm and 1569 nm. As pictured in Figure 4.9 (c), the average output power increased linearly starting from the Q-switched threshold value of 22.4 mW up to the maximum pump power of 114.8 mW. Obtained power values are from 0.04 mW to 0.76 mW at 1529 nm, 0.07 mW to 0.95 mW at 1549 nm, and 0.06 mW to 1.35 mW at 1569 nm. The MWCNTs' relatively higher damage resistance lies in its unique structure of the higher mass density and thicker outer wall tubular structure, and these aspects impact on the absorption of photon per nanotubes and thus expand its capability for generating intense pulses (Ahmad et al., 2014). Figure 4.10 (d) shows the corresponding pulse energies over the wider wavelength range of

1529 nm, 1549 nm, and 1569 nm, which were 15.93 nJ, 27.4 nJ and 52.3 nJ respectively at the maximum pump power of 114.8 mW.

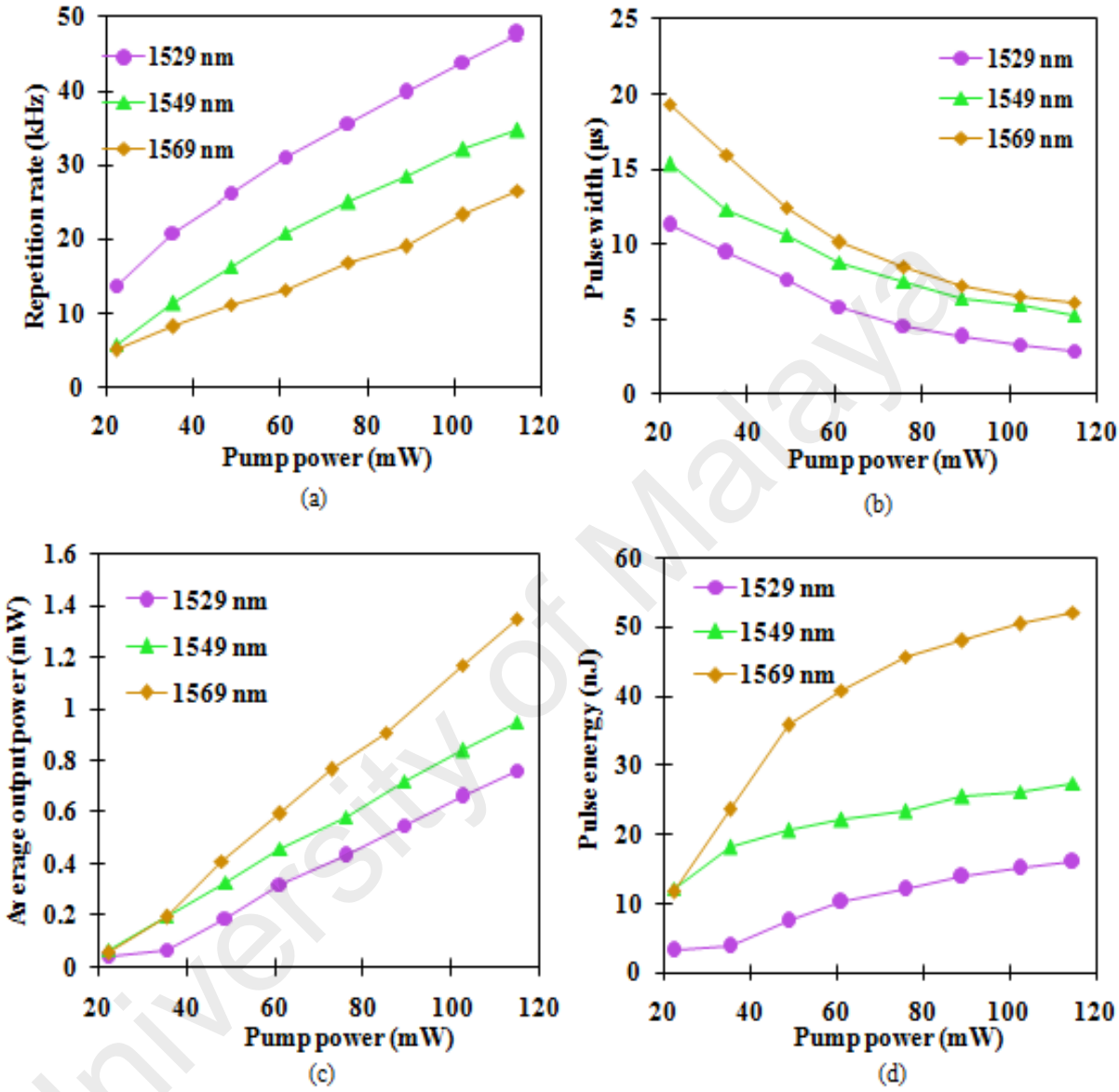

Figure 4.10: Characterization of the MWCNT/PVA-based tunable Q-switched EDFL parameters as functions of pump power, with these parameters being a) repetition rate, b) pulse width, c) average output power, and d) pulse energy.

Figure 4.11 shows the oscilloscope traces of Q-switched pulse train for EDFLs at different wavelengths taken at the maximum pump power of 114.8 mW. The Q-switched pulse train has uniform pulse shapes, along with fluctuations from peak to peak that diminish with increasing wavelength, for different output wavelengths of 1529 nm (Figure 4.11 (a)), 1549 nm (Figure 4.11 (b)), and 1569 nm (Figure 4.11 (c)). There is no distinct amplitude modulation in each Q-switched envelop spectrum, which indicates that self-mode locking effect and pulse jitter effects on Q-switching is suppressed. The laser output exhibited spectral broadening across a wider wavelength that followed the ASE spectrum, whereby the peak wavelength of 1529 nm resulted in the highest pulse repetition rate in comparison with other wavelength of 1549 nm and 1569 nm that were associated with a lower pulse repetition rate. Figure 4.11 (a) indicates the closest pulse spacing with the smallest pulse interval of 20.97 μs at 1529 nm, while Figure 4.11 (b) shows the pulse slightly broadens as the pulse interval increases up to 28.92 μs at 1549 nm. Figure 4.11 (c) depicts the widest spacing between the pulses occurring at 1569 nm as the pulse interval expands to 37.69 μs.

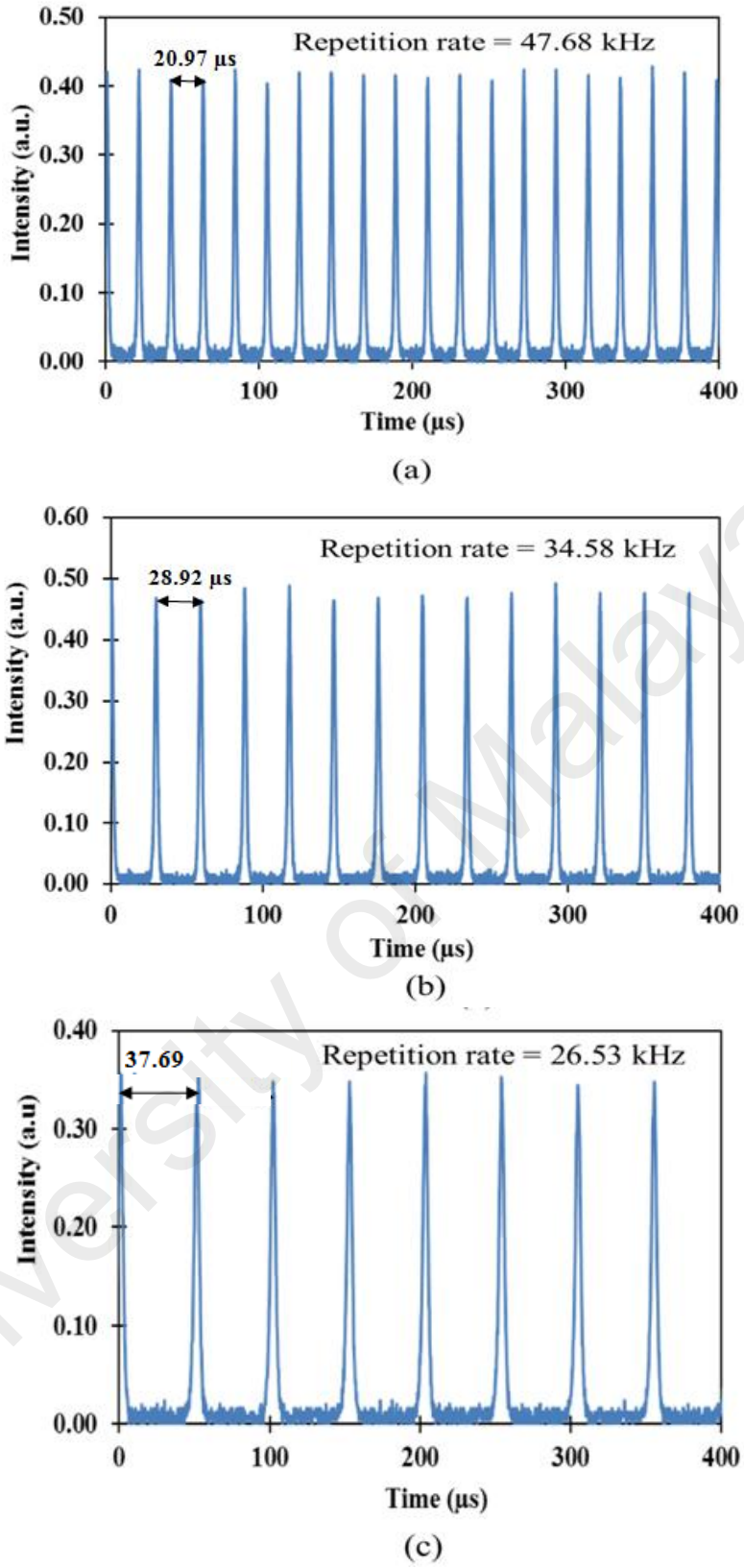

Figure 4.11: Output pulse train at the maximum pump power of ~114.8 mW at different output wavelengths of a) 1529 nm, b)1549 nm and c) 1569 nm

The variation of the repetition rate and pulse width by tuning the TBPF to different wavelengths from 1519 nm to 1569 nm, with pump power fixed at 114.8 mW, is shown in Figure 4.12(a). It can be viewed from this figure that the pulse repetition rate becomes lower as the laser is tuned to longer wavelengths. The outcome indicates that an MWCNT/PVA-based tunable Q-switched EDFL could provide a wide tuning operation spanning from the S-band to C-band region. The pulse repetition rate becomes lower due to the gain difference of the EDF, and the insertion loss in the cavity varies with wavelength, this behavior caused the change in the repetition rate at different wavelengths, as reported by Ahmad et al. (2013).The highest repetition rate achieved was 47.68 kHz, with a corresponding pulse width of 2.83 μs at 1529 nm, whereas the minimum repetition rate was 26.53 kHz, corresponding to a pulse width of 6.10 μs at 1569 nm. The results in Figure 4.12 (b) are indicative of the relationship between average output power and the pulse energy measured against operating wavelength, while pump power remained at the maximum of 114.8 mW. The maximum average output power was 1.35 mW with pulse energy of 52.13 nJ at 1569 nm, and the lowest average output power was 0.76 mW with measured pulse energy of 15.93 nJ at 1529 nm.

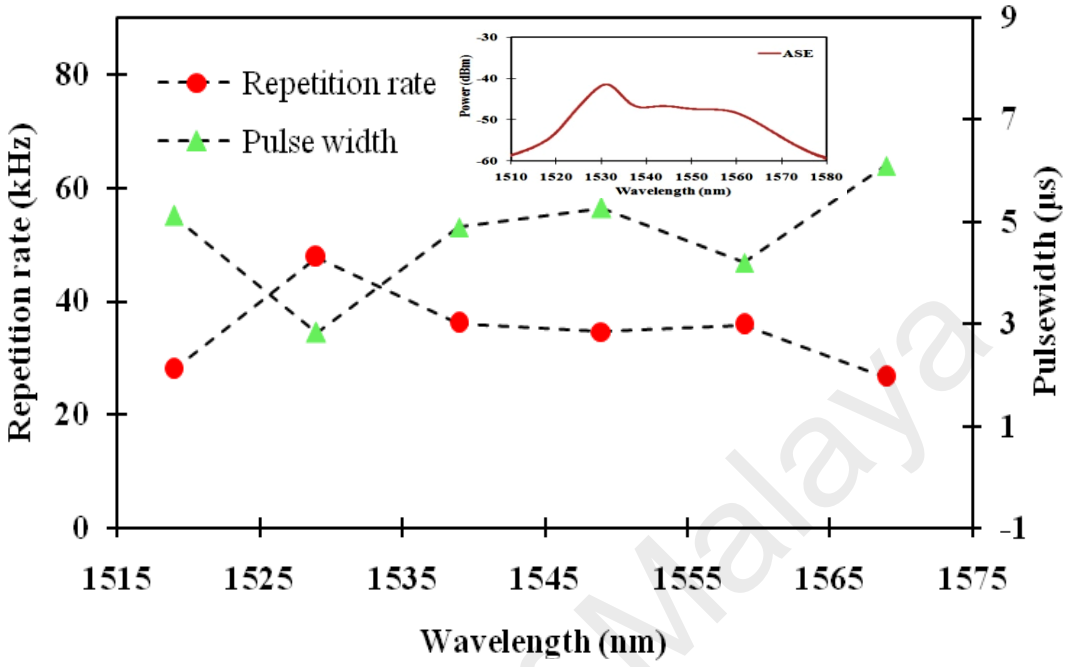

(a)

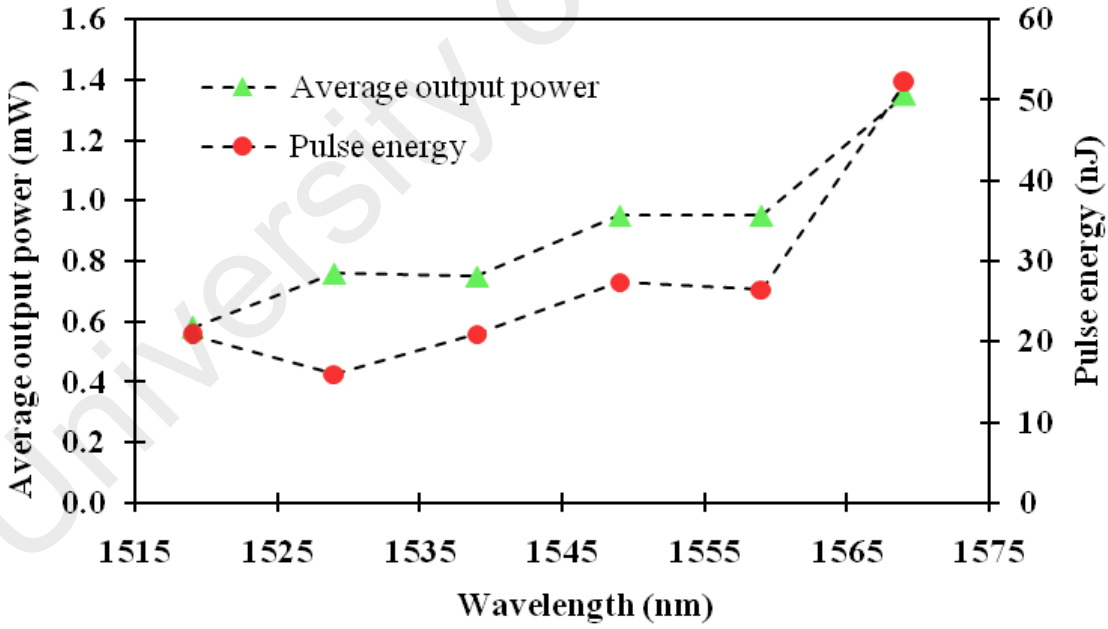

(b)

Figure 4.12: a) Repetition rate and pulse width, and b) Average output power and pulse energy, as function of different output wavelengths

Figure 4.13 displays the results of the stability measurement that was carried out at a pump power of 35.5 mW in order to verify and investigate the stability of the output power and output wavelength of the proposed MWCNT/PVA based Q-switched EDFL. The observation time was 60 minutes with measurements at time intervals of 5 minutes at the center wavelength of 1559 nm and with output power of approximately -4.76 dBm. These results prove that the proposed system is able to maintain its performance, since the variation of output power and wavelength was only about 1.3 dBm and 0.04 nm respectively. Although the measurements are displayed for a period of 60 minutes, the output was observed to remain stable in excess of 180 minutes of test duration.

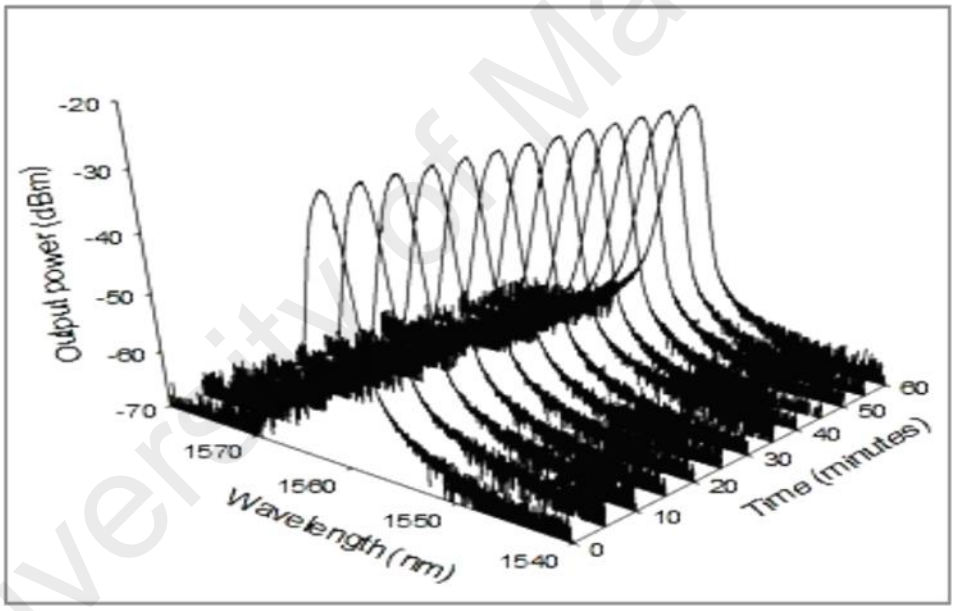

Figure 4.13: Stability measurement of Q-switched operation for 60 minutes with output wavelength 1559 nm at an output power of -4.76 dBm

Figure 4.14 shows the radio-frequency (RF) measurement of fundamental peak at 22 kHz before inserting the filter, measured at pump power 61.2 mW at a corresponding center wavelength of 1559 nm. From this figure, the signal-to-ratio (SNR) of Q-switched fiber laser is approximately 60 dBm, indicating that the Q-switched pulse is in relatively stable regime. Apart from the fundamental and harmonic peaks, there is no other frequency component in the RF spectrum with wider span signifying that the Q-switched pulse produced is stable.

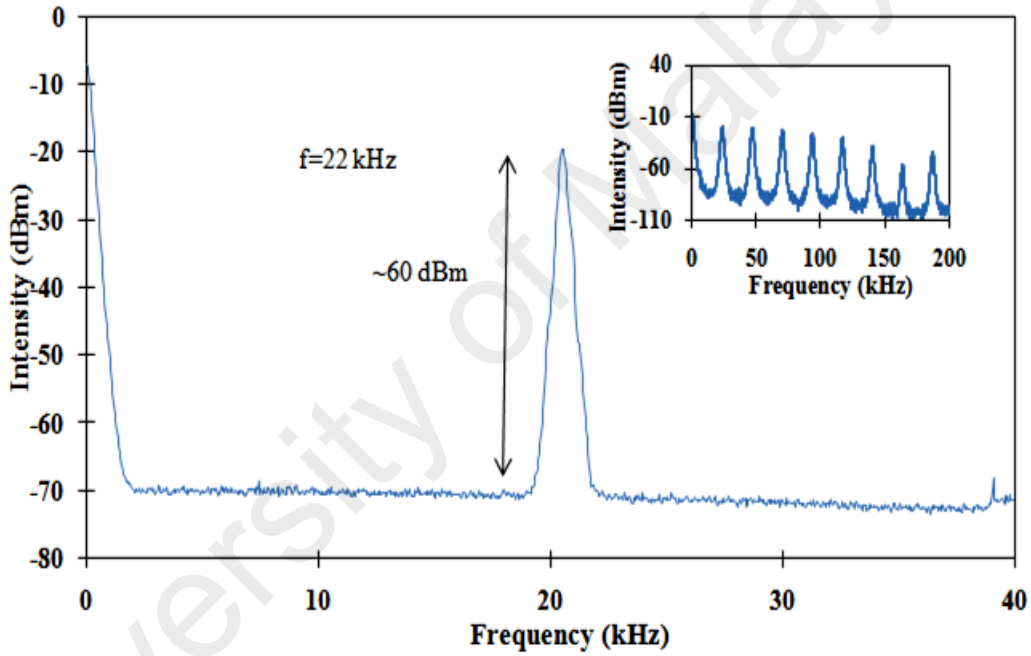

Figure 4.14: RF spectrum of the Q-switched laser with SNR= ~60 dBm, inset graph: the wideband of RF spectrum approximately 200 kHz

CHAPTER 5: CONCLUSION AND RECOMMENDATIONS

5.1 Introduction

This chapter summarizes the results and outcomes of the research work that have been presented in the previous part of this dissertation. The following section provides the conclusion as well as the recommendation for future work.

5.2 Conclusion

5.2.1 The optical properties of the MWCNTs/PVA based saturable absorber.

The first objective of this work, which is to investigate the optical properties of MWCNTs polymer composite based saturable absorber. The cross section of the MWCNTs/PVA film is captured using FESEM image which confirms the MWCNTs are well-dispersed in the PVA matrix. However, the FESEM image does not reveal the structure of MWCNTs distinctly due to the high concentration of PVA polymer.

The Raman spectrum of the MWCNTs/PVA SA exhibits the intensity peaks at Raman shifts approximately 1351 cm^{-1}, 1591 cm^{-1} and 2710 cm^{-1} which correspond to *D, G,* and *G'* bands. The *D* band at 1351 cm^{-1} originates from a double resonance process and is attributed to the presence of amorphous disordered carbon. The G band at 1591 cm^{-1} corresponds to tangential stretching C−C (carbon-carbon) vibrations on the nanotube wall plane , whereas the *G'* peak at 2710 cm^{-1} originates from two-phonon scattering phenomena around the *K* point and around the *M* point in the Brillouin .

Furthermore, an experiment has been carried out to measure the saturable absorption properties of the MWCNTs/PVA saturable absorber. The experimental results enable us to determine the modulation depth, saturation intensity and non-saturable losses of the saturable absorber**.** From the nonlinear saturable absorption measurement, the fabricated

MWCNTs/PVA saturable absorber has a modulation depth of ~6%,a saturation intensity of 0.18 MW/cm^{2}and a non-saturable loss of 91%.

5.2.2 The design of an ultrafast EDFL which employs a MWCNT/PVA-based saturable absorber to generate high energy pulses through Q-switching operation

A stable ultrafast EDFL which employs a MWCNTs/PVA-based SA, which is able to generate high energy pulses Q-switching has been proposed and demonstrated in this work. In the proposed laser, the SA is formed by sandwiching a MWCNTs/PVA film between two ferrules. The SA is then incorporated into an EDFL in a ring configuration to generate a Q-switched laser which operates in the 1.5 μm regions. The MWCNTs are introduced in the PVA host polymer, producing a smoother surface and more uniform thin film compared to the PEO.

Among the tested SA samples, the one with the concentration of 1.25 wt. %, of MWCNTs shows a consistency in generating pulsed laser with a good range of repetition rate, narrowest pulse width and produces a high pulse energy and peak power. Besides showing a good Q-switching performance, the MWCNTs/PVA based saturable absorber is easy to fabricate and requires low cost. This makes the proposed SA a suitable component for passively generating Q-switched laser in the 1.5 micron wavelength region. The maximum repetition rate of 34.3 kHz, shortest pulse width of 3.49 μs, maximum peak power of 11.69 mW and maximum pulse energy of 43.23 nJ, respectively.

5.2.3 A tunable wavelength Q-Switched EDFL with MWCNT/PVA-based saturable absorber

A Q-switched EDFL with MWCNT/PVA based saturable absorber incorporating a tunable bandpass filter (TBPF) was proposed and demonstrated. The TBPF is selected as the wavelength tuning device which also provides a filtering mechanism to achieve a broad wavelength tuning range. The tuning wavelength of the Q-switched pulses covered a wide wavelength range of approximately 50 nm, which spanned from 1519 nm to 1569 nm. In addition, the continuous wave lasing and Q-switching pump threshold were noticeably low, with the values of 15.5mW and 22.4mW respectively.

The measurements of pulse repetition rate, pulse width, average output power and pulse energy against pump power at different operating wavelength of 1529 nm, 1549 nm, and 1569 nm are taken at the maximum pump power of approximately 114.8 mW. The highest pulse repetition rate at output wavelength of 1529 nm is 47.68 kHz with the lowest pulse width of 2.83 μs. The corresponding average output power is 0.76 mW and the pulse energy is 15.93 nJ. At an output wavelength of 1549 nm, the pulse repetition rate and pulse width is giving value of 34.58 kHz and 4.19 μs respectively, whereas the corresponding average output power and the pulse energy is 0.95 mW and 27.4 nJ respectively. The highest pulse energy of 52.13 nJ was obtained at an output wavelength of 1569 nm, with a corresponding repetition rate of 26.53 kHz and pulse width of 6.10 μs. This system is proven to be highly stable and the MWCNTs/PVA SA is capable of facilitating the Q-switched operation which produces pulse output for a wide range of wavelength covering S- to C- band.

5.3 Recommendations

This section proposes several recommendations that can be taken into consideration for future work in order to enhance the properties of the saturable absorber and also to

improve the laser design in order to obtain a better laser output. The recommendations are as follows:

In this work, the passive Q-switched operation obtained by using MWCNT/PVA based saturable absorber is capable to operate in a broad wavelength span (approximately 50 nm) from S-band to C-band. The broadness of the operating wavelength span is influenced by the MWCNTs' diameter distribution. Hence, increasing the number of walls and broadening the diameter distribution of the MWCNT could possibly assist in achieving wider operating range.

Higher dopant (erbium ions) concentration in the EDF could increase the pump absorption. The increase in the pump absorption will result into the built up of larger population inversion which leads to higher gain. Therefore, the length of the laser cavity can be reduced since shorter EDF with higher dopant concentration can be used and consequently imposes minimum loss in the laser cavity. This will provide higher output power and resulting to the generated pulses having higher energy.

In this work, a stable pulse laser generation can be obtained by using polymer composites based film by sandwiching them between two fibre ferrules with an assistance of index-matching gel. However, the film can be easily removed or displaced from the ferrule due to increasing laser intensity, which will end up degrading the laser performance .As an alternative, another approach can be implemented by using the evanescent wave interaction with employment of the tapered fibers or D-shaped fibers into the laser cavity . The benefits are the nonlinear interaction length of the light with the SA will increase and the intensity of the interaction is low, providing higher thermal damage.The output energy of the Q-switched EDFL is expected to improve.

REFERENCES

Ahmad, F., Haris, H., Nor, R. M., Zulkepely, N. R., Ahmad, H., & Harun, S. W. (2014). Passively Q-Switched EDFL Using a Multi-Walled Carbon Nanotube PolymerComposite Based on a Saturable Absorber. Chinese Physics Letters, 31(3). doi: Artn 034204Doi 10.1088/0256-307x/31/3/034204

Ahmad, H., Ismail, M. F., Hassan, S. N. M., Ahmad, F., Zulkifli, M. Z., & Harun, S. W. (2014). Multiwall carbon nanotube polyvinyl alcohol-based saturable absorber in passively Q-switched fiber laser. Applied Optics, 53(30), 7025-7029. doi: Doi 10.1364/Ao.53.007025

Ahmad, H., Muhammad, F. D., Zulkifli, M. Z., & Harun, S. W. (2013). Wideband tunable Q-switched fiber laser using graphene as a saturable absorber. Journal of Modern Optics, 60(18), 1563-1568. doi: Doi 10.1080/09500340.2013.842005

Ahmad, H., Zulkifli, M. Z., Muhammad, F. D., Zulkifli, A. Z., & Harun, S. W. (2013). Tunable graphene-based Q-switched erbium-doped fiber laser using fiber Bragg grating. Journal of Modern Optics, 60(3), 202-212. doi: Doi 10.1080/09500340.2013.766767

Ahmed, M. H. M., Ali, N. M., Salleh, Z. S., Rahman, A. A., Harun, S. W., Manaf, M., & Arof, H. (2015). Q-switched erbium doped fiber laser based on single and multiple walled carbon nanotubes embedded in polyethylene oxide film as saturable absorber. Optics and Laser Technology, 65, 25-28. doi: DOI 10.1016/j.optlastec.2014.07.001

Banhart, F. (1999). Irradiation effects in carbon nanostructures. Reports on Progress in Physics, 62(8), 1181-1221. doi: Doi 10.1088/0034-4885/62/8/201

Becker, P. M., Olsson, A. A., & Simpson, J. R. (1999). Erbium-doped fiber amplifiers: fundamentals and technology: Academic press.

Burrus, C. A., Stone, J., & Dentai, A. G. (1976). Room-temperature 1.3 μm cw operation of a glass-clad Nd: yag single-crystal fibre laser end pumped with a single led. Electronics Letters, 12(22), 600-602.

Cao, W. J., Wang, H. Y., Luo, A. P., Luo, Z. C., & Xu, W. C. (2012). Graphene-based, 50 nm wide-band tunable passively Q-switched fiber laser. Laser Physics Letters, 9(1), 54-58. doi: DOI 10.1002/lapl.201110085

Chakrapani, N., Curran, S., Wei, B., Ajayan, P. M., Carrillo, A., & Kane, R. S. (2003). Spectral fingerprinting of structural defects in plasma-treated carbon nanotubes. Journal of materials research, 18(10), 2515-2521.

Chen, Y., Zhao, C., Chen, S., Du, J., Tang, P., Jiang, G., . . . Tang, D. (2014). Large energy, wavelength widely tunable, topological insulator Q-switched erbium-doped fiber laser. Selected Topics in Quantum Electronics, IEEE Journal of, 20(5), 315-322.

Chen, Y., Zhao, C. J., Chen, S. Q., Du, J., Tang, P. H., Jiang, G. B., . . . Tang, D. Y. (2014). Large Energy, Wavelength Widely Tunable, Topological Insulator Q-Switched Erbium-Doped Fiber Laser. Ieee Journal of Selected Topics in Quantum Electronics, 20(5). doi: Artn 0900508Doi 10.1109/Jstqe.2013.2295196

Digonnet, M. J. F., Gaeta, C. J., & Shaw, H. J. (1986). 1.064-Mu-M and 1.32-Mu-M Nd - Yag Single-Crystal Fiber Lasers. Journal of Lightwave Technology, 4(4), 454-460. doi: Doi 10.1109/Jlt.1986.1074730

Dong, B., Liaw, C. Y., Hao, J. Z., & Hu, J. H. (2010). Nanotube Q-switched low-threshold linear cavity tunable erbium-doped fiber laser. Applied Optics, 49(31), 5989-5992. doi: Doi 10.1364/Ao.49.005989

Elim, H. I., Ji, W., Ma, G. H., Lim, K. Y., Sow, C. H., & Huan, C. H. A. (2004). Ultrafast absorptive and refractive nonlinearities in multiwalled carbon nanotube films. Applied Physics Letters, 85(10), 1799-1801. doi: Doi 10.1063/1.1786371

Han, M. M., Zhang, S. M., Li, X. L., Zhang, H. X., Wen, F., & Yang, Z. J. (2014). High-energy, tunable-wavelengths, Q-switched pulse laser. Optics Communications, 326, 24-28. doi: DOI 10.1016/j.optcom.2014.04.012

Hasan, T., Sun, Z., Tan, P., Popa, D., Flahaut, E., Kelleher, E. J., . . . Torrisi, F. (2014). Double-Wall Carbon Nanotubes for Wide-Band, Ultrafast Pulse Generation. Acs Nano, 8(5), 4836-4847.

Hasan, T., Sun, Z., Wang, F., Bonaccorso, F., Tan, P. H., Rozhin, A. G., & Ferrari, A. C. (2009). Nanotube–polymer composites for ultrafast photonics. Advanced Materials, 21(38-39), 3874-3899.

Hassan, C. M., & Peppas, N. A. (2000). Structure and applications of poly(vinyl alcohol) hydrogels produced by conventional crosslinking or by freezing/thawing methods. Biopolymers/Pva Hydrogels/Anionic Polymerisation Nanocomposites, 153, 37-65.

Huang, J. Y., Huang, W. C., Zhuang, W. Z., Su, K. W., Chen, Y. F., & Huang, K. F. (2009). High-pulse-energy, passively Q-switched Yb-doped fiber laser with AlGaInAs quantum wells as a saturable absorber. Optics Letters, 34(15), 2360-2362.

Ismail, M. A., Ahmad, F., Harun, S. W., Arof, H., & Ahmad, H. (2013). A Q-switched erbium-doped fiber laser with a graphene saturable absorber. Laser Physics Letters, 10(2). doi: Artn 025102Doi 10.1088/1612-2011/10/2/025102

Kamaraju, N., Kumar, S., Kim, Y. A., Hayashi, T., Muramatsu, H., Endo, M., & Sood, A. K. (2009). Double walled carbon nanotubes as ultrafast optical switches. Applied Physics Letters, 95(8). doi: Artn 081106Doi 10.1063/1.3213396

Keller, U. (2003). Recent developments in compact ultrafast lasers. Nature, 424(6950), 831-838. doi: Doi 10.1038/Nature01938

Khin, M. M., Nair, A. S., Babu, V. J., Murugan, R., & Ramakrishna, S. (2012). A review on nanomaterials for environmental remediation. Energy & Environmental Science, 5(8), 8075-8109. doi: 10.1039/C2EE21818F

Kivisto, S., Hakulinen, T., Kaskela, A., Aitchison, B., Brown, D. P., Nasibulin, A. G., . . . Okhotnikov, O. G. (2009). Carbon nanotube films for ultrafast broadband technology. Optics Express, 17(4), 2358-2363. doi: Doi 10.1364/Oe.17.002358

Koester, C. J., and Snitzer, E. (1964).Amplification in a fiber laser, Applied Optics,3(10), pp. 1182–1186.

Kürti, J., Zólyomi, V., Grüneis, A., & Kuzmany, H. (2002). Double resonant Raman phenomena enhanced by van Hove singularities in single-wall carbon nanotubes. Physical Review B, 65(16), 165433.

Laroche, M., Chardon, A. M., Nilsson, J., Shepherd, D. P., Clarkson, W. A., Girard, S., & Moncorge, R. (2002). Compact diode-pumped passively Q-switched tunable Er-Yb double-clad fiber laser. Optics Letters, 27(22), 1980-1982. doi: Doi 10.1364/Ol.27.001980

Lim, S. H., Elim, H. I., Gao, X. Y., Wee, A. T. S., Ji, W., Lee, J. Y., & Lin, J. (2006). Electronic and optical properties of nitrogen-doped multiwalled carbon nanotubes. Physical Review B, 73(4). doi: Artn 045402Doi 10.1103/Physrevb.73.045402

Lin, Y. H., Yang, C. Y., Liou, J. H., Yu, C. P., & Lin, G. R. (2013). Using graphene nano-particle embedded in photonic crystal fiber for evanescent wave mode-

locking of fiber laser. Optics Express, 21(14), 16763-16776. doi: Doi 10.1364/Oe.21.016763

Liu, H., Chow, K., Yamashita, S., & Set, S. (2013). Carbon-nanotube-based passively Q-switched fiber laser for high energy pulse generation. Optics & Laser Technology, 45, 713-716.

Mahad, F. D., Supa'at, M., & Sahmah, A. (2009). EDFA gain optimization for WDM system. Elektrika, 11(1), 34-37.

Maiman, T. H. (1960). Stimulated optical radiation in ruby masers, Nature, vol. 187,pp. 493–494

Nelson, L. E., Jones, D. J., Tamura, K., Haus, H. A., & Ippen, E. P. (1997). Ultrashort-pulse fiber ring lasers. Applied Physics B-Lasers and Optics, 65(2), 277-294. doi: DOI 10.1007/s003400050273

Okhotnikov, O., Grudinin, A., & Pessa, M. (2004). Ultra-fast fibre laser systems based on SESAM technology: new horizons and applications. New Journal of Physics, 6. doi: Artn 177Pii S1367-2630(04)81446-0Doi 10.1088/1367-2630/6/1/177

Popa, D., Sun, Z., Hasan, T., Torrisi, F., Wang, F., & Ferrari, A. C. (2011). Graphene Q-switched, tunable fiber laser. Applied Physics Letters, 98(7). doi: Artn 073106Doi 10.1063/1.3552684

Ramadurai, K., Cromer, C. L., Lewis, L. A., Hurst, K. E., Dillon, A. C., Mahajan, R. L., & Lehman, J. H. (2008). High-performance carbon nanotube coatings for high-power laser radiometry. Journal of Applied Physics, 103(1). doi: Artn 013103Doi 10.1063/1.2825647

Rashid, B. O.,& Jaff, P. M.(2008). Gain and Noise Figure Performance of Erbium-Doped Fiber Amplifiers at 10Gbps Kirkuk University Journal Scientific Studies 60.

Reilly, R. M. (2007). Carbon nanotubes: potential benefits and risks of nanotechnology in nuclear medicine. Journal of Nuclear Medicine, 48(7), 1039-1042.

Rosdin, R. Z., Ahmad, R. R., Ali, F., N. M., Harun, S. W.,& Arof, H.(2014). Q-switched Er-doped fiber laser with low pumping threshold using graphene saturable absorber, Chinese Optic Letter, 12 091404.

Saito, R., Jorio, A., Souza Filho, A., Dresselhaus, G., Dresselhaus, M., & Pimenta, M. (2001). Probing phonon dispersion relations of graphite by double resonance Raman scattering. Physical review letters, 88(2), 027401.

Schibli, T. R., Minoshima, K., Kataura, H., Itoga, E., Minami, N., Kazaoui, S., . . . Sakakibara, Y. (2005). Ultrashort pulse-generation by saturable absorber mirrors based on polymer-embedded carbon nanotubes. Optics Express, 13(20), 8025-8031. doi: Doi 10.1364/Opex.13.008025

Set, S. Y., Yaguchi, H., Tanaka, Y., & Jablonski, M. (2004a). Laser mode locking using a saturable absorber incorporating carbon nanotubes. Journal of Lightwave Technology, 22(1), 51-56. doi: Doi 10.1109/Jlt.2003.822205

Set, S. Y., Yaguchi, H., Tanaka, Y., & Jablonski, M. (2004b). Ultrafast fiber pulsed lasers incorporating carbon nanotubes. Ieee Journal of Selected Topics in Quantum Electronics, 10(1), 137-146. doi: Doi 10.1109/Jstqe.2003.822912

Siegman, A. E. (1986). Lasers University Science Books. Mill Valley, CA, 37

Skorczakowski, M., Swiderski, J., Pichola, W., Nyga, P., Zajac, A., Maciejewska, M., . . Bragagna, T. (2010). Mid-infrared Q-switched Er:YAG laser for medical applications. Laser Physics Letters, 7(7), 498-504. doi: DOI 10.1002/lapl.201010019

Snitzer, E. (1961). Optical maser action of Nd^{+3} in a barium crown glass, Physical Review Letters, 7, pp. 444–446.

Sun, Z., Hasan, T., & Ferrari, A. C. (2012). Ultrafast lasers mode-locked by nanotubes and graphene. Physica E-Low-Dimensional Systems & Nanostructures, 44(6), 1082-1091. doi: DOI 10.1016/j.physe.2012.01.012

Sun, Z. P., Hasan, T., Torrisi, F., Popa, D., Privitera, G., Wang, F. Q., . . . Ferrari, A. C. (2010). Graphene Mode-Locked Ultrafast Laser. Acs Nano, 4(2), 803-810. doi: Doi 10.1021/Nn901703e

Wang, F., Rozhin, A. G., Sun, Z., Scardaci, V., Penty, R. V., White, I. H., & Ferrari, A. C. (2008). Fabrication, characterization and mode locking application of single-walled carbon nanotube/polymer composite saturable absorbers. International Journal of Material Forming, 1(2), 107-112. doi: DOI 10.1007/s12289-008-0371-y

Williams, R. J., Jovanovic, N., Marshall, G. D., & Withford, M. J. (2010). All-optical, actively Q-switched fiber laser. Optics Express, 18(8), 7714-7723. doi: Doi 10.1364/Oe.18.007714

Xinju, L. (2010). Laser technology: CRC press.

Yamashita, S., Inoue, Y., Hsu, K., Kotake, T., Yaguchi, H., Tanaka, D., . . . Set, S. Y. (2005). 5-GHz pulsed fiber Fabry-Perot laser mode-locked using carbon nanotubes. Ieee Photonics Technology Letters, 17(4), 750-752.

Yu, J. R., Grossiord, N., Koning, C. E., & Loos, J. (2007). Controlling the dispersion of multi-wall carbon nanotubes in aqueous surfactant solution. Carbon, 45(3), 618-623. doi: DOI 10.1016/j.carbon.2006.10.010

Zhang, H., Tang, D. Y., Knize, R. J., Zhao, L. M., Bao, Q. L., & Loh, K. P. (2010). Graphene mode locked, wavelength-tunable, dissipative soliton fiber laser. Applied Physics Letters, 96(11). doi: Artn 111112Doi 10.1063/1.3367743

Zhang, L., Wang, Y. G., Yu, H. J., Sun, L., Hou, W., Lin, X. C., & Li, J. M. (2011). Passive mode-locked Nd:YVO4 laser using a multi-walled carbon nanotube saturable absorber. Laser Physics, 21(8), 1382-1386. doi: Doi 10.1134/S1054660x11150333

Zhang, L. Q., Zhuo, Z., Wang, J. X., & Wang, Y. Z. (2012). Passively Q-switched fiber laser based on graphene saturable absorber. Laser Physics, 22(2), 433-436. doi: Doi 10.1134/S1054660x12020284

Zhao, H. M., Lou, Q. H., Zhou, J., Zhang, F. P., Doug, J. X., Wei, Y. R., & Wang, Z. J. (2007). Stable pulse-compressed acousto-optic Q-switched fiber laser. Optics Letters, 32(19), 2774-2776. doi: Doi 10.1364/Ol.32.002774

Zhou, D. P., Wei, L., Dong, B., & Liu, W. K. (2010). Tunable Passively Q-switched Erbium-Doped Fiber Laser With Carbon Nanotubes as a Saturable Absorber. Ieee Photonics Technology Letters, 22(1), 9-11. doi: Doi 10.1109/Lpt.2009.2035325

Zhou, S. A., Ouzounov, D. G., & Wise, F. W. (2006). Passive harmonic mode-locking of a soliton Yb fiber laser at repetition rates to 1.5 GHz. Optics Letters, 31(8), 1041-1043. doi: Doi 10.1364/Ol.31.001041

LIST OF PUBLICATIONS AND PAPERS PRESENTED

1) Ahmad, H., **Hassan,S. N. M**., Ahmad, F., Zulkifli, M. Z., &Harun, S. W. (2016). Broadband tuning in a passively Q-switched erbium doped fiber laser (EDFL) via multiwall carbon nanotubes/polyvinyl alcohol (MWCNT/PVA) saturable absorber. Optics Communications, *365*, 54-60.

2) Ahmad, H., Ismail, M. F., **Hassan, S. N. M**., Ahmad, F., Zulkifli, M. Z., & Harun, S. W. (2014). Multiwall carbon nanotube polyvinyl alcohol-based saturable absorber in passively Q-switched fiber laser.Applied optics, 53(30), 7025-7029.

3) Ahmad, H., Ismail, M. F., **Hassan, S. N. M**., Muhammad, F. D., Zulkifli, M. Z., & Harun, S. W. (2014). Supercontinuum generation from a sub-megahertz repetition rate femtosecond pulses based on nonlinear polarization rotation technique. Journal of Modern Optics, 61(16), 1333-1338.

- 2014 - Conference at International Seminar on Photonics, Optics and its application (ISPhOA 2014) in Bali entitled ‘Nitrogen-doped graphene as a saturable absorber for passively Q-switched fiber laser.
- 2015 - Conference at 10th International Symposium on Modern Optics and Its Applications (ISMOA’15) Bandung,Indonesia entitled "High energy pulse in passively Q-switched using MWCNT/PVA as a saturable absorber".